(E84-10170) THE NEAR-EARTH MAGNETIC FIELD AT 1980 DETERMINED FROM MAGSAT DATA (NASA) 61 p HC A04/MF A01 CSCL 05B

N84-31733

Unclas
G3/43 00170

NASA

Technical Memorandum 86133

THE NEAR-EARTH MAGNETIC FIELD AT 1980 DETERMINED FROM MAGSAT DATA

R. A. Langel
and
R. H. Estes

August 1984

National Aeronautics and
Space Administration

Goddard Space Flight Center
Greenbelt, Maryland 20771

The Near-Earth Magnetic Field at 1980 Determined from Magsat Data

R.A. Langel[1]

Bullard Laboratories
University of Cambridge
Madingley Rise, Madingley Road,
Cambridge CB3 0EZ, U.K.

R.H. Estes

Business and Technological Systems
Seabrook, Md. 20801,
U.S.A.

[1] On sabbatical from Goddard Space Flight Center, Greenbelt, Md., 20991, USA

Abstract

Data from the Magsat spacecraft for November 1979 through April 1980 and from 91 magnetic observatories for 1978 through 1982 are used to derive a spherical harmonic model of the earth's main magnetic field and its secular variation at epoch 1980.0. The model is called GSFC(12/83). Constant coefficients are determined through degree and order 13 and secular variation coefficients through degree and order 10. The first degree external terms and corresponding induced internal terms are given as a function of Dst. Preliminary modeling using separate data sets at dawn and dusk local time showed that the dusk data contains a substantial field contribution from the equatorial electrojet current. The final data set was therefore selected first from dawn data and then augmented by dusk data to achieve a good geographic data distribution for each of three time periods: (1) November - December, 1979; (2) January - February, 1980; (3) March - April, 1980. A correction for the effects of the equatorial electrojet was applied to the dusk data utilized. The solution included calculation of fixed biases, or anomalies, for the observatory data. Although similar in many respects, GSFC(12/83) differs from IGRF 1980 by 3.6 nT in the g_1^0 term and shows a slightly negative $\dot{B}$ in the northern polar region as well as other differences in secular variation pattern.

Introduction

NASA's Magsat spacecraft has provided the first truly global vector survey of the near-earth geomagnetic field. Data from early in the mission have previously been used to study the main (i.e. originating in the earth's core) field in terms of an initial model (Langel et al., 1980), the spectral distribution of the field (Langel & Estes, 1982) and as part of the data used in the 1960-1980 model of Langel et al. (1982a) which was one of the candidates for the 1980 International Geomagnetic Reference Field (IGRF). Since these early results the entire Magsat data set has been processed and a careful selection made of data suitable for modeling the main field. The present paper describes our best estimate of that main field derived from the final Magsat data.

Characteristics of the Magsat spacecraft, its instrumentation and its operation have been published previously (Acuna et al. 1978; Mobley et al., 1980; Lancaster et al., 1980; Langel et al., 1981, 1982b). The resulting vector data span the interval November 1979 through April 1980. After final attitude corrections and calibrations the data are estimated to be accurate to about 6nT (nanotesla) rss in each component and 2nT rss in field magnitude. This includes all known sources of error, including those of spacecraft position and attitude determination. The altitude range of the data is about 300-500 km. Orbital parameters were chosen so that Magsat was sun-synchronous at the terminator (i.e. the day-night boundary) so data are acquired

only at dusk and dawn local times.

The field is assumed to be curl-free and so representable by a potential function in the form of the usual spherical harmonic series:

$$V = r_o \sum_{n=1}^{NMAX1} \sum_{m=o}^{n} (r_o/r)^{n+1} [g_n^m \cos m\varphi + h_n^m \sin m\varphi] P_n^m(\cos\vartheta)$$

$$+ r_o \sum_{n=1}^{NMAX2} \sum_{m=o}^{n} (r/r_o)^n [q_n^m \cos m\varphi + s_n^m \sin m\varphi] P_n^m(\cos\vartheta) \qquad (1)$$

where r_o is the mean radius of the earth, taken to be 6371.2 km, r, ϑ and φ are the standard spherical coordinates and $p_n^m(\cos\vartheta)$ are the Schmidt quasi-normalised form of associated Legendre functions. The magnetic field is then given by

$$\vec{B} = -\nabla V. \qquad (2)$$

Theoretically (1) holds only if NMAX1 and NMAX2 go to infinity and when the region of validity is source free. The measured internal $\vec{B}$ contains contributions both from the Earth's core and

from its crust and NMAX1 is chosen so that V represents fields from the core but not the crust, to our best estimation. Langel and Estes (1982) concluded that the core field dominates for $n < 13$ and the crustal field for $n > 15$ so, as in Langel et al. (1980 and 1982a), we have chosen NMAX1 = 13. Because Magsat passes through regions of "field aligned" currents, the source free assumption does not strictly hold. These currents have minimal effect on the field magnitude (Langel, 1974) so our procedure is to use the component data equatorward, but only the field magnitude poleward, of 50° geomagnetic latitude.

The main contribution to the external portion of (1) comes from the equatorial ring current, with contributions also from magnetopause and magnetotail currents. Near the earth, fields from these sources tend to be aligned mainly along the dipole axis and so are well described when NMAX2 = 1. However, unlike the field from the core, the external fields vary considerably with both universal and local time. The hourly Dst index is commonly taken to be an indicator of the relative change of these fields. Accordingly, Langel and Estes (1984) have investigated the relationship between q_1° and Dst, which accounts for the universal time variation of q_1°. It's local time variation was investigated by carrying out the analysis separately for dawn and dusk giving the relationships:

$$\text{Dusk:} \quad q_1^{\circ} = 20.3 - 0.68\ \text{Dst} \quad (\text{nT}) \qquad (3a)$$

$$\text{Dawn:} \quad q_1^{\,o} \approx 18.62 - 0.63\ \text{Dst} \quad (\text{nT}) \tag{3b}$$

Similar relationships will hold at local times inaccessible to Magsat. These are discussed using data from the POGO spacecraft in a later section of this paper. Because the external fields are time varying there are corresponding induced currents within the earth which, in turn, contribute to the internal potential, e.g. $g_1^{\,o}$. Accordingly $g_1^{\,o}$ is expressed as a constant core field plus an induced internal field proportional to $q_1^{\,o}$:

$$\text{Dusk:} \quad g_1^{\,o} = -29987.7 + 0.24\ q_1^{\,o} \quad (\text{nT}) \tag{4a}$$

$$\text{Dawn:} \quad g_1^{\,o} = -29992.3 + 0.29\ q_1^{\,o} \quad (\text{nT}) \tag{4b}$$

For greater validity in representation the present model includes relationships like (3) and (4), but omitting the local time dependance.

Comparison of Dawn and Dusk results

Division of the Magsat data into dawn and dusk subsets furnishes two independent data sets. Differences between models derived from these data sets should be an indication of the effects of local time asymmetries in external fields as well as in data quality and should also give some indication of the accuracy to which the spherical harmonic coefficients are deter-

mined. The data sets for dawn and dusk described by Langel and Estes (1984) were modified slightly to improve geographic coverage and to eliminate a few data with apparent external field effects. Their analysis was then repeated with nearly identical results.

From equation (4) it is clear that there is a difference of about 5nT in the g_1^0 term. Table 1 shows differences between coefficients of the amended models, up to degree/order five. Substantial differences in constant coefficients are present, especially for g_1^0, g_3^0, g_5^0, h_3^1 and g_5^1, and the secular variation coefficients show even larger discrepancies. Differences of this magnitude were totally unexpected and are too large to be due to data inaccuracy. A plot of the component differences indicates that the equatorial electrojet is the chief cause of the discrepancy. Plots of the dusk field minus the dawn field for the X (north) and Z (down) component are shown in Figures 1a and b. The dominant feature is a positive ridge in X following the geomagnetic equator with flanking positive Z to the north and negative Z to the south. This is precisely the result one would expect if the equatorial electrojet, which is eastward and below the spacecraft, were present at dusk and not at dawn. That the electrojet is present at dusk and not dawn is also found in our examination of individual and averaged passes in connection with studies of crustal fields and in the analysis of Roy (1983) who explicitly isolates and models the electrojet field. Maeda et al. (1982) and Roy (1983) also find

variations in the Y (east) component at dusk only, which they attribute to meridional currents.

Figure 1 also shows a large dawn-dusk difference in the Antarctic (about 120° longitude, - 75° latitude) whose source, presumably ionospheric currents associated with the auroral belt, we are unable to identify with certainty.

To model the field from the earth's core free from equatorial electrojet effects requires either exclusive use of dawn data at the affected latitudes or correction of the dusk data. We chose the latter option because it made the final data distribution significantly better. The ideal correction would probably be a dynamic model of the equatorial electrojet. In the absence of any adequate model we resorted to the expedient of using the difference between the dawn and dusk potentials as the correction. Such a correction was applied to B and X between ± 20° geomagnetic latitude, to Y between ± 15° geomagnetic latitude and to Z between ± 50° geomagnetic latitude. It should be recognized that this correction removes a great deal of the independance of the dawn and dusk data sets. The model derived from this data set is referred to as the corrected dusk model.

Columns 5 and 8 of Table 4 show the differences between the dawn and corrected dusk models and figures 2a and b show the new differences between calculated X and Z components. The coefficient differences no longer show isolated large values and are of amplitude in accord with the expected data accuracy. They should give some indication of the accuracy to which the

coefficients are determined. The difference plots no longer show evidence of the equatorial electrojet (as expected from the nature of the correction) but the higher latitude differences are still present.

Final Data Selection

Because the model includes the secular variation it was necessary to obtain a good data distribution both in space and time. Accordingly, after careful selection to ensure the data were from magnetically quiet periods (Langel and Estes, (1984) , the data were separated into three intervals: (1) November-December, 1979; (2) January-February, 1980; (3) March-April, 1980. For each period, and for dawn and dusk data separately, the data were collected into $5^{\circ} \times 5^{\circ}$ equiangular bins over the globe. In regions with geomagnetic latitude equatorward of 50° where vector data with final attitude corrections were not available, field magnitude data were used from data whose attitude was known to a lesser accuracy. Residuals were computed from the GSFC(9/80) model (Langel et al, 1982) and outlying points rejected. Within each bin data having outlying residuals relative to the mean for the bin were also rejected.

Data from each bin were then selected so as to obtain roughly the same number of points per equal area at all latitudes and to maintain an adequate spread of Dst values between $\pm$ 22.5 nT to facilitate the external field analysis.

Priority of selection went to the dawn data with dusk data added to augment the spatial coverage. Dusk data within the "correction region" previously discussed were given a high weighting factor as were a few passes of lesser quality which were added to complete the geographic coverage. Also a few vector points were selected from quiet polar cap data and added to the data set. Table 2 shows the distribution of selected data by component, local time and time period.

Two versions of this data set were used: one with the correction applied to the dusk data and one with no correction.

Preliminary modeling with the combined data set indicated that secular variation coefficients determined from Magsat data alone were significant only up to degree and order four. (This model is available upon request). Also, the coefficients so determined differ significantly enough from the 1980 IGRF that we were unsure of their reliability. (See also Cain et al., 1983.) Accordingly we supplemented the Magsat data with the annual means from 91 observatories for the period 1978-1982. As described by Langel et al. (1982), the model included a solution for parameters representing the non-core field, or anomaly bias, at each observatory. Table 3 lists the observatories used together with the anomaly bias from the solution and the difference between this anomaly bias and that from the GSFC(9/80) model. Data from each observatory were used after converting to X, Y and Z components in a geodetic coordinate system assuming an equatorial radius of 6398.165 km and reciprocal

flattening of 298.25. The spatial distribution of the observatories is displayed in Figure 4. The observatory data were taken from the NOAA National Geophysical and Solar Terrestrial Data Center release 30 annual means data, with some updates for recently acquired data. This data set differs in some respects from the NOAA release 22 data set (updated by the authors) which was used for the GSFC(9/80) model in that the NOAA Data Center applied corrections to some observatories to account for discontinuities. Because of this some observatory biases in the present model differ from those for the GSFC(9/80) model. The observatories for which this is true are Alibag, Baker Lake, Bangui, Barrow, Bereznayki, Dikson and Kakioka. Only the observatories College, Fredericksburg, Guam, Honolulu, M'Bour, Maputo, Pamatai, and San Juan had five annual means for the interval 1978.5 through 1982.5. Thirty-six observatories had four and the remainder three annual means.

The Model

The modeling method used is described in Langel et al. (1982).

Both "corrected" and "uncorrected" models were derived but only the "corrected" version, called GSFC(12/83), will be presented here. Differences between the two were of the same magnitude as the difference between the dawn and corrected dusk models.

The external field coefficients for GSFC(12/83) (not as a

function of local time since we have combined all data) are:

$$q_1^{\,0} = 18.4 - 0.63 \text{ Dst (nT)} \qquad (5a)$$

$$q_1^{\,1} = -1.1 - 0.06 \text{ Dst (nT)} \qquad (5b)$$

$$s_1^{\,1} = -3.3 + 0.17 \text{ Dst (nT)} \qquad (5c)$$

The corresponding $g_1^{\,0}$ internal coefficient, including the effects of currents induced by the time-varying external field, is:

$$g_1^{\,0} = -\ 29991.6 + 0.270\ q_1^{\,0} \text{ (nT)} \qquad (6)$$

Note that the Dst variation is determined only for the range - 20 nT < Dst < 20 nT and may not hold outside this range. The corresponding induced contributions to $g_1^{\,1}$ and $h_1^{\,1}$ are regarded as negligible and not computed.

Coefficients for the internal field at 1980 are given in Table 4 along with the standard error determined in the fit and the difference between the dawn and corrected dusk model. We have contended before (Langel et al., 1982) that the standard errors of the coefficients as determined by the fitting process tend to under-estimate the coefficient inaccuracy. There are several possible reasons for this, such as deficiencies in the model validity, improper estimates of data correlation, and systematic effects of non-core fields. From Table 4, differences between dawn and dusk models are generally greater than the

standard error of the coefficients. In the present case the two data sets should have identical error characteristics, except for the effects of unaccounted for fields from ionospheric and magnetospheric current systems. We expect, then, that the coefficient standard errors reflect the internal consistency of the data whereas the differences between dusk and dawn models reflect the magnitude of the error from these external current systems. Table 5 summarizes the relative magnitude of the two sources. In general the estimated standard errors are too low by at least a factor of 2-3, perhaps about a factor of 5 overall. The additional error tends to occur at lower degree and, from examination of Table 4, within a particular degree at lower order. That is, the source is of long rather than short wavelength. Errors estimated on the basis of the coefficient differences may still be somewhat underestimated because of the loss of independence in the corrected dusk model.

Secular variation terms up to degree and order ten are listed in Table 6 together with the standard error of the coefficients. These coefficients are determined in a two step process wherin coefficients found insignificant in the first step are constrained to zero in the second step. (This procedure was not necessary for the main field model, all coefficients were significant.) Differences between the degree and order four dawn and corrected dusk secular variation models were generally a factor of three or less larger than the corresponding standard errors. No such independant error estimate is available for the

final model incorporating the observatory data, but presumably the factor is similar.

Table 7 gives the statistics of the various data sets relative to GSFC(12/83). The Magsat data used are before any selection required to achieve equal area distribution and so include more data than used in the model determination. As expected, the residuals are higher for the dusk data. The mean value of 4.3 nT in Y in the dusk data (and the 1.3 nT in the merged data) is due to the meridional current discovered by Maeda et al. (1982). The mean value of -4.6 nT in Z in the dawn data (and the -3.7 nT in the merged data) is as yet unaccounted for.

Discussion

Comparison of the GSFC(12/83) coefficients with those of earlier Magsat based models, including IGRF 1980, shows that the principal differences are the addition of the more accurate external field representation and of the secular variation determination. This is not to say that the small changes in constant coefficients are totally insignificant but rather that their effect is only seen in studies of small amplitude phenomena such as some of the details of crustal anomalies. An equally accurate independent data set is required to assess adequately the increased accuracy of this model. Because of the availability of separate dawn and dusk data sets it was possible to give some idea of actual coefficient accuracy but this was impaired by the necessity of correcting the dusk data for the effects of the equatorial electrojet. Contour maps of the various components at 1980 are virtually indistinguishable from those of the IGRF (Peddie, 1982).

For a model commensurate with the accuracy of the Magsat data inclusion of a model of external fields is a requirement. Table 8 gives a comparison of the g_1^0 term from MGST(6/80), GSFC(9/80) and IGRF 1980. Only MGST(6/80) included a determination of q_1^0 and it did not include variation with Dst or take into account that some of g_1^0 could arise from induced currents. The g_1^0 difference between GSFC(9/80) (and IGRF 1980) and GSFC(9/80) is about -3.6 nT. If due totally to fields from induced currents this corresponds to a q_1^0 of 13.3 nT and a Dst

of 8.0 nT. The g_1^o difference between MGST(6/80) and GSFC(12/83) is much smaller.

For some users of the model it may be desirable to take into account the local time variation of q_1^o. Langel and Estes (1984) found that for data from the POGO spacecraft:

$$q_1^o = a + b\ Dst \qquad (7)$$

where a and b both varied with local time. The values of a at dawn and dusk were in disagreement with those from Magsat data but the values of b were in good agreement. It is suggested therefore that the expression for b from Langel and Estes be used in those applications where local time variations of q_1^o are important. That value is given by

$$b = 0.680 + 0.134 \sin (t + 13^o), \qquad (8)$$

where t is the local time in degrees.

Recent examination of the Magsat data shows several small amplitude features which differ between local times but are relatively persistent for a particular local time. It is therefore conceivable that a more detailed external field model is possible than that set forth here.

To our knowledge the only previously published secular variation models for 1980 are GSFC(9/80) (Langel et al. 1982a), that of Barraclough et al. (1982), that of Peddie and Fabiano (1982), the IGRF 1980 (Peddie, 1982) and M061581 (Cain et al., 1983). GSFC(9/80), while a good model for 1960-1980, is not suitable for prediction and will not be considered. IGRF 1980 is a combination of the models of Peddie and Fabiano (1982) and

Barraclough et al. (1982) and in our estimation is a good predictive model. Rather than considering each of these three models we will discuss only IGRF 1980,

Cain et al. (1983) investigated the use of Magsat data, supplemented by linear trends derived from quiet day midnight values at 19 observatories over the November 1979 to June 1980 interval, in the determination of secular variation. They made a comparison of $\dot{B}$ between M061581 and IGRF 1980. The largest discrepancy is in the northern polar region where M061581 is strongly negative whereas IGRF 1980 is slightly positive. They attribute the difference to the effect of seasonal changes in external fields on the secular variation terms in M061581 and point out the possible importance of the effects of earth currents induced by changes in external current systems and of ionospheric currents below the satellite.

$\dot{B}$ as derived from the degree/order four Magsat models (see earlier paragraph) also shows negative values at the northern pole. These are, however, greatly reduced in amplitude compared to M061581 (-20 to -40 nT/yr compared to -70 to -100 nT/yr), presumably because the external field was more accurately accounted for in our model. Figure 3 shows plots of secular variation for the various components from GSFC(12/83). Comparison with plots from the IGRF (Peddie, 1982) shows a general agreement. There are, however, differences in some details. The cell of large $\dot{B}$ in the Atlantic off of the Southeast Coast of the U.S. has intensified by approximately 10

nT/year and shifted slightly to the northeast. Also there has been a decrease in $\dot{B}$ over most of Europe of approximately 20 nT/year. The pattern in the northern polar region closely resembles the structure of the degree/order four Magsat models discussed above. The zero nT/year contour extends to only the eastern coast of Greenland and turns back over the Asian Arctic region, leaving the north polar region more negative (by approximately 20 nT/year) than indicated by IGRF 1980. Comparison of $\dot{Z}$ shows a decrease of approximately 20 nT/year over central Asia, and a more complicated structure near the magnetic equator in the Pacific basin. The high positive cell off the coast of Equador has decreased in magnitude by 40 nT/year and moved to the east. To the east of New Zealand, an intensification in $\dot{Y}$ of approximately 20 nT/year has appeared. The high negative $\dot{X}$ cell in the South Atlantic has intensified with an east-west signature, causing the region of low negative values off of the west coast of South America to disappear.

The high accuracy of the constant coefficients determined from Magsat data does not extend to the secular variation model. Compared to IGRF 1980, GSFC(12/83) has the advantage of greater availability of observatory data spanning 1980 and of the availability of a good (albeit short) temporal distribution of Magsat data. Statistics of the observatory data versus GSFC(12/83) are given in Table 7. Comparable statistics versus IGRF 1980 are found in Table 9. To make the two comparable, observatory "anomaly bias" values from GSFC(12/83) were used in both cases.

As expected the GSFC(12/83) model is a better representation of the data.

Figures 5(a) - 5(c) show the yearly averages at a series of observatories together with the field predicted by GSFC(12/83) and IGRF 1980. These figures are fairly typical of the set of observatories used in the solution. On the whole, the secular variation trends predicted by the models are in close agreement. However it is clear that GSFC(12/83) benefits from the use of more recent data in defining the secular variation after 1980. The $\dot{Z}$ variation of GSFC(12/83) at Muntinlupa (Figure 5(d)) shows the result of taking data over a short time interval when one of the annual means is not in agreement with the longer term trend. The secular variation solution is sensitive to the weights given the observatory data in the least squares adjustment. An initial model derived using the set of observatory weights from GSFC(9/80) produced first degree secular variation coefficients $\dot{g}_1^0 = 23.3$, $\dot{g}_1^1 = 13.8$, $\dot{h}_1^1 = -20.9$ and much less accurate secular variation trends at the observatories than the GSFC(12/83) model, which assigns a weight for each component at each observatory based on the standard deviation of a linear fit to the data over only the 1978-1982 interval.

It is instructive to plot some of the spherical harmonic coefficients of secular variation from the various models available in the literature as a function of time. In doing so we have tried to avoid selecting "predictive" models, i.e. models which are not based on data spanning the applicable interval,

except for IGRF 1980. This eliminates several models for which the input data was graphically projected to a future epoch and it requires assigning a modified epoch to secular variation models based on data from a period of time earlier than the epoch of the associated main field model. Figure 6 contains plots of $\dot{g}_1^{\,o}$, $\dot{g}_2^{\,o}$, $\dot{h}_1^{\,1}$ and $\dot{h}_2^{\,1}$ for the 1960-1980 time period from the models listed in Table 10. The dashed lines on the Figures are drawn by hand. The variation of $\dot{g}_1^{\,o}$ shows a change in slope (i.e. in secular acceleration) near 1968. The nature of the trend after 1968 is unclear; there is some indication of a negative trend but if GSFC(12/83) is correct the trend could either be constant or negative followed by positive. Since $g_1^{\,o}$ is the term most affected by solar cycle variations, perhaps there is a sunspot cycle variation (short dashes) superposed on the long term trend (long dashes).

A sharp change in trend is evident in $\dot{g}_2^{\,o}$ at 1971, after which the coefficient magnitude decreases sharply. A similar sharp change occurs in the $\dot{h}_2^{\,1}$ trend at 1971. These sharp changes in secular acceleration are further corroboration of the "1970 jerk" described, e.g., by Ducruix et al. (1980), Le Mouel et al. (1982), Malin et al. (1983) and Gubbins (1984). From Figure 6 we can obtain estimates of the secular acceleration and its change. For $g_2^{\,o}$ the pre- and post-1971 secular accelerations are about -0.18 nT/yr^2 and +0.80 nT/yr^2. Corresponding values for $h_2^{\,1}$ are +1.0 nT/yr^2 and -1.2 nT/yr^2. These values differ somewhat from those of Malin et al. (1983) but are in good agree-

ment with those of Gubbins (1984). The relation of the 1968 change in $\dot{g}_1^{\,o}$ to the "jerk" is unclear. (Note, the values given by Malin et al. (1983) should be divided by four due to an algebraic error (Malin, private communication) which brings them into closer agreement.)

Computation of "anomaly bias" values for observatory data was introduced by Langel et al. (1982) in an attempt to take into account the fields from crustal anomalies at observatory locations together with any possible observer or instrumental bias. If no change in bias source occurs the bias should not change with time or from model to model. In practice, ability to determine accurately such a bias depends upon the adequacy of the model for the description of the true core field and its secular variation. For example suppose f(t) varies with time as:

$$f(t) = b(t - t_o) + c(t - t_o)^2 \tag{9}$$

and we try to model f(t) with

$$g(t) = a' + b' (t - t_o) \tag{10}$$

That is, f(t) has quadratic time dependance and no "bias" whereas the model is deficient in that it includes no quadratic time dependance but does include a bias. If f(t) is measured over the interval $t_o - s/2$ to $t_o + s/2$ and the square difference of f(t) and g(t) is minimized with respect to a' and b' over this

interval, then the solutions for a' and b' are b' = b and a' = $(cs^2)/12$. Thus, the inadequate model results in a false bias.

Table 3 gives the difference in bias determination between GSFC(9/80) and GSFC(12/83) for those observatories common to both. Note that the time periods over which the two determinations were made are disjoint as the GSFC(9/80) model included observatory annual means only through 1977. The rms of these differences are given in Table 11 for each component together with the rms of the actual biases determined in the GSFC(9/80) model. Because the temporal variation over the four year time span of the GSFC(12/83) model is a great deal less complicated than that for the 20 year time span of the GSFC(9/80) model we expect that the temporal model of GSFC(12/83) should be more accurate. This leads us to conclude that the biases determined in the GSFC(12/83) model are probably more accurate. The differences are greater than we had expected and if they are an indication of model error rather than of a change at the observatory, then we are representing the local bias only to about 15%. The large change in the Y bias at Bereznayki is related to a jump in the data which occurs at 1976.5, and the differences in bias values at Luanda Belas are related to the very rapid change in the data at 1981.5. These results may be caused by a site or instrument change or a change in procedures. The cause of these and other large differences is under investigation.

REFERENCES

Acuna, M.H., C.S. Scearce, J.B. Seek and J. Scheifele, The Magsat vector magnetometer - A precision fluxgate magnetometer for the measurement of the geomagnetic field, NASA/GSFC TM79656, October 1978.

Barraclough, D.R., J.M. Harwood, B.R. Leaton and S.R.C. Malin, A definitive model of the geomagnetic field and its secular variation for 1965-I. Derivation of model and comparison with IGRF, Geophys. J. R. astr. Soc., 55, 111-121, 1978.

Barraclough, D.R., B.M. Hodder and S.R.C. Malin, The IGS proposal for the New International Geomagnetic Reference Field, J. Geomag. Geoelectr., 34, 351-356, 1982.

Cain, J.C., J. Frayser, L. Muth and D. Schmitz, The use of Magsat data to determine secular variation, J. Geophys. Res., 88, 5903-5910, 1983.

Ducruix, J., V. Courtillot and J.Le Mouel, The late 1960s secular variation impulse, the eleven year magnetic variation and the electrical conductivity of the deep mantle, Geophys. J.R. astr. Soc., 61, 73-94, 1980.

Gubbins, D., Geomagnetic field analysis - II. Secular variation consistent with a perfectly conducting core, accepted for publication in Geophys J.R. astr. Soc., 77, 1984.

Hurwitz, L. and E.B. Fabiano, Geomagnetic secular variation 1937.5-1967.5, unpublished manuscript, August 1969.

Hurwitz, L., D.G. Knapp, E.B. Fabiano and N.W. Peddie, Geomagnetic secular change, 1964-1970, from satellite F and observatory X, Y and Z, Jour Geophys. Res., 78, 8351-8355, 1973.

Hurwitz, L., E.B. Fabiano and N.W. Peddie, A model of the geomagnetic field for 1970. Jour. Geophys. Res., 79, 1716-1717, 1974.

Lancaster, E.R., T. Jennings, M. Morrissey and R.A. Langel, Magsat vector magnetometer calibration using Magsat geomagnetic field measurements, NASA/GSFC TM82046, November 1980.

Langel, R.A., Near-earth magnetic disturbance in total field at high latitudes 1. Summary of data from Ogo 2, 4 and 6, J. Geophys. Res., 79, 2363-2371, 1974

Langel, R.A. and R.H. Estes, A geomagnetic field spectrum, Geophys. Res. Lett. 9, 250-253, 1982.

Langel, R.A. and R.H. Estes, Large-scale, near-earth, magnetic fields from external sources and the corresponding induced internal field, J. Geophys. Res., to appear, 1984.

Langel, R.A., R.H. Estes, G.D. Mead, E.B. Fabiano and E.R. Lancaster, Initial geomagnetic field model from Magsat vector data, Geophys. Res. Lett., 7, 793-796, 1980.

Langel, R., J. Berbert, T. Jennings and R. Horner, Magsat data processing: A report for investigators, NASA/GSFC TM82160, November, 1981

Langel, R.A., R.H. Estes and G.D. Mead, Some new methods in geomagnetic field modeling applied to the 1960-1980 epoch, J. Geomag. Geoelectr., 34, 327-349, 1982a.

Langel, R., G. Ousley, J. Berbert, J. Murphy and M. Settle, The Magsat Mission, Geophys. Res. Lett., 9, 243-245, 1982b

Le Mouel, J., J. Ducruix and Chau Ha Duyen, The worldwide character of the 1969-1970 impulse of the secular acceleration rate, Phys. Earth and Planet Int., 28, 337-350, 1982.

Maeda, H., T. Iyemori, T. Araki and T. Kamei, New evidence of a meridional current system in the equatorial ionosphere, Geophys. Res. Lett. 9, 341-344, 1982.

Malin, S.R.C., Geomagnetic secular variation and its changes, Geophys. J.R. astr. Soc. 17, 415-441, 1969.

Malin, S.R.C., B.M. Hodder and D.R. Barraclough, Geomagnetic secular variation: a jerk in 1970, Publicado en volumen conmemorativo 75 aniversario del observatorio del Ebro, pg 239-256, Roquetes, 1983.

Mobley, F.F., L.D. Eckard, G.H. Fontain and G.W. Ousley, Magsat - A new satellite to survey the earth's magnetic field, IEEE Trans., on magnetics, 16, 758-760, 1980.

Peddie, N.W., International Geomagnetic Reference Field, the third generation, J. Geomag. Geoelectr., 34, 309-326, 1982.

Peddie, N.W. and E.B. Fabiano, A model of the geomagnetic field for 1975, Jour. Geophys. Res., 81, 2539-2542, 1976.

Peddie, N.W. and E.B. Fabiano, A proposed International Geomagnetic Reference Field for 1965-1985, J. Geomag. Geoelectr., 34, 357-364, 1982.

Roy, M., Equatorial Ionospheric currents derived from Magsat data, Preprint, 1983.

Table 1: Difference between coefficients from the dawn spherical harmonic model and the dusk spherical harmonic model up to degree and order five

n	m	Δg_n^m	Δh_n^m	$\Delta \dot{g}_n^m$	$\Delta \dot{h}_n^m$
1	0	4.80	0.0	-2.26	0.0
1	1	-0.19	-0.08	2.65	3.21
2	0	0.87	0.0	2.50	0.0
2	1	0.20	0.13	-2.80	0.77
2	2	-0.06	-0.06	1.96	-0.68
3	0	-3.36	0.0	0.88	0.0
3	1	-0.06	-1.08	0.45	3.27
3	2	0.09	-0.03	-1.31	0.60
3	3	-0.91	0.25	-1.02	-0.10
4	0	0.40	0.0	-2.95	0.0
4	1	0.42	0.36	0.33	-2.62
4	2	0.45	0.13	2.57	-1.88
4	3	-0.03	-0.21	0.71	0.15
4	4	-0.50	0.22	-2.24	1.77
5	0	1.70	0.0	0.0	0.0
5	1	0.25	-1.86	0.0	0.0
5	2	-0.45	-0.31	0.0	0.0
5	3	0.17	0.11	0.0	0.0
5	4	0.06	0.13	0.0	0.0
5	5	-0.42	0.13	0.0	0.0

Table 2: Number of measurements in final merged Data Sets

Merged Data		Nov-Dec	Jan-Feb	March-April
X	Dawn	2320	2591	2596
	Dusk	1833	1609	1620
Y	Dawn	2251	2457	2419
	Dusk	1902	1775	1797
Z	Dawn	2778	3255	3404
	Dusk	1375	948	812
B	Dawn	2975	2882	3251
	Dusk	2680	2605	2593

Table 3: Observatories Used in the Model

Station	Lat.	Long.	Alt.	Anomaly bias (nT) X	Y	Z	Bias Differences with GSFC(9/80) X	Y	Z
ABISKO	68.36	18.82	0.37	19.3	54.6	29.7			
ADDIS ABABA	9.03	38.76	2.44	507.3	-27.6	119.8	17.8	-42.7	-28.9
ALERT	82.50	-62.50	0.06	-6.1	31.2	-197.5	-11.8	-3.4	-54.3
ALIBAG	18.64	72.87	0.0	-207.1	457.9	594.4	-126.9	-5.8	-74.6
ALMA ATA	43.25	76.92	1.30	148.6	37.8	-183.8	22.7	-4.4	-31.7
ALMERIA	36.85	-2.46	0.06	-14.3	17.5	5.4	-8.3	8.9	-16.8
AMATSIA	31.55	34.92	0.0	105.0	38.2	273.1			
ANNAMALAINAGAR	11.37	79.68	0.0	178.8	-90.3	-59.5	-40.7	-9.9	115.1
AQUILA	42.38	13.32	0.62	-1.3	37.5	-3.1	7.1	-4.7	-12.6
ARGENTINE ISLND	-65.24	-64.26	0.0	68.3	-74.6	486.7	-1.0	8.9	-26.1
BAKER LAKE	64.33	-96.03	0.04	161.5	-47.1	-92.4	-57.9	62.6	21.9
BANGUI	4.44	18.57	0.38	-148.3	-26.1	222.9	-29.0	-62.7	115.6
BARROW	71.32	-156.62	0.0	21.6	-69.7	-55.4	-2.3	-3.6	-23.4
BELSK	51.84	20.79	0.18	107.7	132.3	298.7	11.2	-21.2	-15.3
BEREZNAYKI	49.82	73.08	0.0	-379.6	-193.2	310.6	44.2	-207.9	-28.3
BJORNOYA	74.50	19.20	0.07	-110.0	57.4	18.0	12.1	10.3	-10.0
BOULDER	40.14	-105.24	1.65	-14.2	50.6	-166.8	38.3	-2.9	-6.5
CAMBRIDGE BAY	69.20	-105.00	0.02	102.7	-96.9	116.1			
CASEY	-66.28	110.53	0.0	906.2	-307.9	-669.4			
CHAMBON FORET	48.02	2.26	0.14	-71.8	-21.7	103.8	7.9	2.9	-15.2
COIMBRA	40.22	-8.42	0.09	21.3	-5.5	5.3	26.7	17.3	-42.7
COLLEGE	64.86	-147.84	0.09	-18.0	-55.5	-106.8	-0.8	5.2	0.5
DIKSON	73.54	80.56	0.01	-85.0	-133.7	-262.8	19.5	13.9	-14.2
DOURBES	50.10	4.60	0.20	4.0	-16.6	81.8	11.7	0.2	-16.6
DUMONT DURVILLE	-66.66	140.01	0.03	-150.1	-405.8	-2861.2	41.9	-13.5	-8.3
DUSHETI	42.09	44.71	0.98	-221.5	6.5	-114.5	16.9	1.7	-31.8
ESKDALEMUIR	55.32	-3.20	0.24	4.7	-49.4	-52.6			
FORT CHURCHILL	58.77	-94.10	0.04	-116.5	31.6	-269.0	23.7	-15.2	-13.2
FREDERICKSBURG	38.21	-77.37	0.06	56.9	-63.9	135.4	28.8	5.8	14.9
FURSTNFELDBRUCK	48.16	11.28	0.57	-24.8	-8.3	12.1	6.4	-2.4	-2.8
GNANGARA	-31.78	115.95	0.06	-3.4	-126.7	142.3	47.6	1.1	19.8
GORNOTAYEZHNAYA	43.68	132.17	0.30	-8.9	-11.2	-62.2	4.4	12.3	-24.4
GREAT WHALE R	55.27	-77.78	0.02	261.0	102.0	-79.7	2.7	-11.5	-20.8
GUAM	13.58	144.87	0.15	133.6	86.2	76.6	-41.3	-18.1	79.3
HARTLAND	50.99	-4.48	0.09	-42.6	11.6	62.2	12.0	4.6	-2.0
HERMANUS	-34.43	19.23	0.02	18.2	11.3	24.5	35.8	-12.7	30.2
HONOLULU	21.32	-158.00	0.0	-167.5	80.1	-340.9	6.9	-32.8	-36.3
HUANCAYO	-12.04	-75.34	3.31	69.4	36.1	17.5	-20.9	-12.4	-229.3
HYDERABAD	17.41	78.55	0.49	305.3	20.8	476.5	-46.9	-88.8	19.5
KAKIOKA	36.23	140.19	0.02	-11.8	10.4	-86.6	-5.0	7.3	-22.3
KANOYA	31.42	130.88	0.10	-15.1	55.3	-37.3			
KERGUELEN	-49.35	70.20	0.04	223.0	189.8	643.4	45.8	-16.3	10.4
KODAIKANAL	10.23	77.46	2.32	-548.8	287.9	-32.1			
LEIRVOGUR	64.18	-21.70	0.0	-285.1	601.3	-488.5	14.8	6.4	-5.6
LERWICK	60.13	-1.18	0.08	-127.2	169.9	35.5	10.1	0.6	-2.2
LOVO	59.35	17.83	0.02	44.8	-4.8	-3.5	9.6	-5.7	-11.0
LUANDA BELAS	-8.92	13.17	0.05	290.5	-30.1	204.8	97.5	-23.7	154.3
LUNPING	25.00	121.17	0.10	6.6	45.7	40.0	-9.4	80.3	-39.9
LVOV	49.90	23.75	0.20	140.2	121.4	146.3	11.3	-3.9	-7.4
M BOUR	14.39	-16.96	0.0	119.9	46.8	53.5	-23.1	95.2	-25.3
MACQUARIE ISLND	-54.50	158.95	0.0	274.3	2.4	292.8	38.0	9.7	-16.7
MAPUTO	-25.92	32.58	0.05	349.7	34.0	-137.3			
MAWSON	-67.60	62.88	0.0	23.3	21.9	182.0	6.6	-3.1	-15.7
MEANOOK	54.62	-113.33	0.67	118.4	12.6	-142.0	50.5	4.3	18.3
MEMAMBETSU	43.91	144.19	0.03	-243.4	141.9	65.1	-4.1	8.8	-12.1
MIRNYY	-66.55	93.02	0.02	-102.9	48.3	-450.1	32.2	-1.9	-21.6
MOULD BAY	76.20	-119.40	0.15	-20.9	-1.6	-65.3	1.5	-6.6	-24.6
MUNTINLUPA	14.38	121.01	0.06	-44.1	-44.5	35.4	20.1	139.4	16.3
NAGYCENK	47.63	16.72	0.15	15.0	-5.6	-51.0			
NEWPORT	48.26	-117.12	0.77	-38.8	111.1	-122.0	32.5	0.9	6.2
NIEMEGK	52.07	12.68	0.07	-31.9	-1.4	-82.4	9.4	-1.5	-14.4
NURMIJARVI	60.51	24.65	0.11	281.8	-106.1	95.3	10.7	-7.8	-11.9
OTTAWA	45.40	-75.55	0.76	133.9	-146.5	157.3	29.2	-3.5	-27.4

Table 3: Observatories Used in the Model

Station	Lat.	Long.	Alt.	Anomaly bias (nT) X	Y	Z	Bias Differences with GSFC(9/80) X	Y	Z
PAMATAI	-17.57	-149.57	0.09	-664.5	-732.2	-127.7	11.3	-40.7	82.0
PLESHENITZI	54.50	27.88	0.20	275.8	171.7	-139.8	6.4	23.4	-20.2
PORT MORESBY	-9.41	147.15	0.08	11.5	49.3	273.3	51.7	-10.5	109.9
PORT-ALFRED	-46.43	51.87	0.0	-696.4	1187.7	153.9			
QUETTA	30.19	66.95	1.75	-8.4	83.2	-54.7	2.9	32.5	-0.1
RESOLUTE BAY	74.70	-94.90	0.03	45.2	29.0	56.1	9.5	-1.1	-15.9
SABHAWALA	30.36	77.80	0.49	-19.6	-63.9	15.0	-4.4	-36.1	-48.0
SAN JUAN	18.11	-66.15	0.40	-50.9	170.4	183.8	88.4	-4.6	-29.8
SANAE	-70.30	-2.37	0.05	-24.7	8.7	14.5	26.7	27.8	-14.1
SITKA	57.06	-135.32	0.02	-5.4	-19.8	-67.2	6.2	-5.3	15.7
SODANKYLA	67.37	26.63	0.17	-159.4	-106.4	-589.9	5.2	-2.1	-11.0
ST JOHN S	47.60	-52.68	0.0	57.2	22.6	-8.0	48.2	-3.9	-5.9
SURLARI	44.68	26.25	0.08	10.3	-32.1	-69.1			
THULE II	77.48	-69.17	0.05	-63.4	103.5	5.0	-7.5	-1.4	-8.3
TIHANY	46.90	17.89	0.19	-26.8	6.9	-43.8	-10.2	23.4	-16.1
TOLEDO	39.88	-4.05	0.50	9.7	4.4	-3.0			
TRIVANDRUM	8.48	76.95	0.29	276.7	204.1	210.3	21.7	8.9	137.3
TROMSO	69.66	18.95	0.11	110.1	-407.3	117.1	54.6	-5.8	-80.5
TSUMEB	-19.22	17.70	0.08	53.0	-68.0	115.6	58.9	-8.0	52.6
TUCSON	32.25	-110.83	0.76	-61.1	-59.0	133.2	55.0	3.1	-33.9
VALENTIA	51.93	-10.25	0.0	134.2	-46.0	19.3	15.9	10.1	-6.1
VANNOVSKAYA	37.95	58.11	0.57	170.1	96.4	64.6	-1.4	3.0	5.8
VASSOURAS	-22.40	-43.65	0.45	78.0	-60.5	-35.0	33.5	66.0	36.9
VICTORIA	48.52	-123.42	0.19	31.8	1.7	-327.5	49.4	8.3	0.7
WHITESHELL	49.75	-95.25	0.0	182.3	-242.5	-230.1			
WINGST	53.74	9.07	0.04	55.3	43.1	-66.5	10.9	-3.0	-11.8
WITTEVEEN	52.81	6.67	0.01	23.5	-0.2	-78.2			
YELLOW-KNIFE	62.40	-114.50	0.18	401.2	-216.0	129.7			

Table 4.: The GSFC(12/83) field model

a) Coefficients for Epoch 1980, Units are nT. mean radius of the earth is 6371.2 km

n	m	g_n^m	Standard error	Dawn-Dusk Difference	h_n^m	standard error	Dawn-Dusk Difference
1	0	-29991.6	0.05	-0.80			
1	1	-1956.0	0.08	-0.41	5603.9	0.08	-0.80
2	0	-1996.7	0.05	-0.83			
2	1	3027.3	0.05	-0.31	-2129.3	0.05	-0.10
2	2	1662.7	0.07	-0.03	-199.7	0.07	0.08
3	0	1281.4	0.05	0.33			
3	1	-2180.5	0.06	0.16	-335.5	0.06	0.44
3	2	1250.9	0.05	0.14	270.9	0.05	-0.06
3	3	832.9	0.06	0.15	-252.2	0.06	-0.09
4	0	937.6	0.05	-0.20			
4	1	782.3	0.05	-0.17	212.2	0.05	-0.37
4	2	397.9	0.05	-0.07	-256.7	0.05	-0.07
4	3	-418.9	0.05	0.11	52.9	0.05	0.12
4	4	198.9	0.06	0.13	-297.2	0.06	-0.07
5	0	-217.9	0.05	0.03			
5	1	357.2	0.05	0.09	46.0	0.05	0.67
5	2	261.0	0.05	0.40	149.8	0.05	0.14
5	3	-74.3	0.05	0.05	-150.6	0.05	-0.09
5	4	-161.9	0.05	0.01	-77.7	0.05	-0.04
5	5	-48.0	0.06	0.16	92.1	0.06	-0.06
6	0	48.0	0.05	0.23			
6	1	65.5	0.05	0.29	-14.8	0.05	-0.34
6	2	41.9	0.05	-0.04	93.1	0.05	-0.26
6	3	-192.1	0.05	-0.06	70.6	0.05	0.10
6	4	3.6	0.05	0.02	-43.1	0.05	-0.03
6	5	13.8	0.05	-0.01	-2.2	0.05	-0.06
6	6	-107.7	0.06	-0.02	17.2	0.06	-0.03
7	0	71.9	0.05	-0.53			
7	1	-59.2	0.05	-0.14	-82.5	0.05	0.87
7	2	1.7	0.05	0.54	-27.4	0.05	0.53
7	3	20.7	0.05	0.06	-4.9	0.05	-0.30
7	4	-12.4	0.05	-0.16	16.3	0.05	-0.05
7	5	0.6	0.05	0.08	17.8	0.05	-0.05
7	6	10.6	0.05	0.01	-23.0	0.05	-0.03
7	7	-1.7	0.06	0.08	-9.7	0.05	-0.02
8	0	18.5	0.05	-0.06			
8	1	6.5	0.05	0.26	6.8	0.05	-0.14
8	2	-0.4	0.05	-0.01	-17.7	0.05	-0.3[illegible]
8	3	-11.0	0.05	-0.08	4.2	0.05	-0.0[illegible]
8	4	-6.9	0.05	-0.04	-22.2	0.05	0.00
8	5	4.2	0.05	-0.04	9.1	0.05	-0.02
8	6	2.7	0.05	-0.03	16.1	0.05	-0.00
8	7	6.0	0.05	0.04	-13.2	0.05	-0.01
8	8	-1.4	0.06	-0.01	-14.6	0.06	-0.05
9	0	5.3	0.05	0.28			
9	1	10.4	0.05	0.18	-20.8	0.05	0.06
9	2	1.4	0.05	0.27	15.5	0.05	0.28
9	3	-12.3	0.05	0.13	8.7	0.05	-0.25
9	4	9.4	0.05	-0.10	-5.3	0.05	-0.14
9	5	-3.4	0.05	-0.00	-6.3	0.05	0.09
9	6	-1.2	0.05	0.01	9.0	0.05	0.07
9	7	6.7	0.05	0.09	9.6	0.05	0.07
9	8	1.5	0.05	0.08	-6.0	0.05	-0.03
9	9	-5.0	0.06	-0.02	2.0	0.06	-0.03

Table 4 Cont'd

n	m	g_n^m	Standard error	Dawn-Dusk Difference	h_n^m	standard error	Dawn-Dusk Difference
10	0	-3.5	0.05	-0.23			
10	1	-4.0	0.05	0.07	1.2	0.05	0.24
10	2	2.2	0.05	0.06	0.5	0.05	-0.17
10	3	-5.4	0.05	-0.14	2.7	0.05	-0.04
10	4	-2.0	0.05	0.02	5.8	0.05	-0.01
10	5	4.6	0.05	-0.01	-4.2	0.05	-0.05
10	6	3.1	0.05	-0.03	-0.4	0.05	0.02
10	7	0.9	0.05	0.02	-1.3	0.05	0.08
10	8	2.0	0.05	-0.08	3.6	0.05	-0.04
10	9	2.8	0.05	0.02	-0.5	0.05	0.04
10	10	-0.3	0.00	-0.01	-6.1	0.06	-0.03
11	0	2.5	0.05	0.14			
11	1	-1.1	0.05	0.10	0.6	0.05	-0.12
11	2	-1.7	0.05	0.05	1.7	0.05	0.15
11	3	2.2	0.05	0.15	-1.3	0.05	-0.02
11	4	0.1	0.00	0.04	-3.1	0.05	-0.19
11	5	-0.6	0.05	0.05	0.8	0.05	0.03
11	6	-0.3	0.05	0.01	-0.0	0.05	0.02
11	7	1.6	0.05	0.10	-2.5	0.05	0.02
11	8	1.7	0.05	0.08	-0.4	0.05	0.01
11	9	-0.8	0.05	-0.00	-1.7	0.05	-0.09
11	10	2.0	0.05	-0.01	-1.5	0.05	0.01
11	11	3.4	0.06	-0.02	0.8	0.06	-0.01
12	0	-1.7	0.05	-0.12			
12	1	-0.1	0.05	-0.12	0.2	0.05	0.20
12	2	-0.3	0.05	0.22	0.8	0.05	-0.05
12	3	-0.2	0.05	-0.05	2.5	0.05	-0.02
12	4	0.7	0.05	-0.02	-1.5	0.05	-0.05
12	5	0.6	0.05	-0.02	0.4	0.05	-0.03
12	6	-0.4	0.05	0.00	0.2	0.05	0.05
12	7	-0.2	0.05	-0.00	-0.2	0.05	0.08
12	8	0.3	0.05	-0.03	0.0	0.00	0.02
12	9	-0.5	0.05	0.03	-0.0	0.00	0.02
12	10	0.1	0.00	-0.01	-1.2	0.05	-0.03
12	11	0.6	0.05	0.02	0.4	0.05	-0.04
12	12	-0.1	0.00	0.02	0.5	0.06	-0.06
13	0	-0.2	0.00	0.10			
13	1	-0.6	0.05	0.03	-0.5	0.05	-0.03
13	2	0.4	0.05	0.08	0.3	0.05	0.10
13	3	-0.9	0.05	0.14	1.5	0.05	-0.01
13	4	-0.2	0.00	0.06	-0.2	0.05	-0.11
13	5	1.1	0.05	0.05	-0.5	0.05	-0.03
13	6	-0.4	0.05	-0.05	-0.2	0.00	0.08
13	7	0.4	0.05	0.09	0.8	0.05	0.06
13	8	-0.5	0.05	0.06	0.1	0.00	0.04
13	9	0.2	0.05	0.02	0.9	0.05	-0.08
13	10	-0.1	0.05	-0.03	0.1	0.00	0.03
13	11	0.3	0.05	0.01	-0.1	0.00	0.09
13	12	-0.1	0.00	0.03	0.3	0.00	0.04
13	13	0.4	0.06	0.03	-0.3	0.06	-0.04

Table 5: Comparison of coefficient standard error with dawn-dusk coefficient difference

Degree	Rms of standard error (nT)	Rms of Dawn-Dusk Difference (nT)	Ratio
1	0.07	0.69	9.9
2	0.06	0.40	6.7
3	0.06	0.23	3.8
4	0.05	0.17	3.4
5	0.05	0.25	5.0
6	0.05	0.16	3.2
7	0.05	0.34	6.8
8	0.05	0.11	2.2
9	0.05	0.15	3.0
10	0.05	0.10	2.0
11	0.05	0.08	1.6
12	0.05	0.08	1.6
13	0.04	0.06	1.5

Table 6 : The GSFC(12/83) secular variation model

a) Coefficients for Epoch 1980, Units are nT/yr mean radius of the earth is 6371.2 km

n	m	$\dot{g}_n^m$	Standard error	Dawn-Dusk Difference	$\dot{h}_n^m$	standard error	Dawn-Dusk Difference
1	0	26.5	0.17	1.66			
1	1	11.9	0.23	-0.83	-16.0	0.20	-1.37
2	0	-17.8	0.15	-1.03			
2	1	3.6	0.16	1.00	-15.0	0.19	0.29
2	2	3.1	0.22	-1.15	-24.2	0.22	0.10
3	0	1.2	0.13	-0.03			
3	1	-3.6	0.15	-0.49	2.3	0.15	-2.44
3	2	-1.1	0.17	0.10	2.5	0.15	0.02
3	3	1.8	0.20	0.61	-4.1	0.22	0.03
4	0	-0.7	0.14	0.92			
4	1	-2.1	0.13	0.29	2.9	0.14	1.49
4	2	-5.8	0.15	-1.93	2.0	0.14	0.77
4	3	-2.4	0.15	-0.83	2.0	0.16	0.29
4	4	-2.8	0.25	0.69	-2.4	0.19	0.07
5	0	0.0	0.00	0.00			
5	1	-0.0	0.00	0.00	1.4	0.15	0.00
5	2	-1.3	0.12	0.00	0.5	0.13	0.00
5	3	-4.1	0.13	0.00	-1.0	0.14	0.00
5	4	-1.3	0.17	0.00	0.6	0.15	0.00
5	5	0.0	0.00	0.00	0.1	0.17	0.00
6	0	1.6	0.12	0.00			
6	1	0.4	0.09	0.00	0.4	0.10	0.00
6	2	1.0	0.11	0.00	-0.7	0.10	0.00
6	3	1.3	0.09	0.00	0.0	0.00	0.00
6	4	0.6	0.15	0.00	-0.4	0.12	0.00
6	5	0.8	0.10	0.00	0.4	0.13	0.00
6	6	1.6	0.14	0.00	1.6	0.16	0.00
7	0	1.4	0.10	0.00			
7	1	-0.7	0.08	0.00	-0.9	0.12	0.00
7	2	0.3	0.09	0.00	0.8	0.09	0.00
7	3	-0.0	0.00	0.00	0.4	0.10	0.00
7	4	0.8	0.10	0.00	0.2	0.10	0.00
7	5	-0.0	0.00	0.00	0.4	0.12	0.00
7	6	-0.0	0.00	0.00	0.4	0.12	0.00
7	7	1.8	0.16	0.00	-0.0	0.00	0.00
8	0	0.7	0.10	0.00			
8	1	0.0	0.00	0.00	-0.6	0.11	0.00
8	2	0.3	0.09	0.00	-0.0	0.00	0.00
8	3	-0.0	0.00	0.00	0.0	0.00	0.00
8	4	-0.9	0.10	0.00	-0.0	0.00	0.00
8	5	0.3	0.08	0.00	0.7	0.09	0.00
8	6	0.0	0.00	0.00	-0.9	0.08	0.00
8	7	-0.0	0.00	0.00	-0.0	0.00	0.00
8	8	-2.2	0.15	0.00	-1.7	0.19	0.00
9	0	-0.3	0.11	0.00			
9	1	0.0	0.00	0.00	0.5	0.08	0.00
9	2	0.5	0.08	0.00	-0.0	0.00	0.0
9	3	0.0	0.00	0.00	0.9	0.09	0.00
9	4	0.0	0.00	0.00	0.6	0.07	0.00
9	5	-0.1	0.06	0.00	-0.0	0.00	0.00
9	6	0.0	0.00	0.00	-0.0	0.00	0.00
9	7	-0.0	0.00	0.00	-0.0	0.00	0.00
9	8	-0.4	0.11	0.00	0.4	0.10	0.00
9	[illegible]	-1.1	0.16	0.00	2.1	0.16	0.00

Table 6 Cont'd

n	m	g_n^m	Standard error	Dawn-Dusk Difference	h_n^m	standard error	Dawn-Dusk Difference
10	0	0.9	0.07	0.00			
10	1	0.0	0.00	0.00	-0.5	0.07	0.00
10	2	-0.5	0.05	0.00	-0.0	0.00	0.00
10	3	-0.3	0.06	0.00	-0.5	0.07	0.00
10	4	0.7	0.06	0.00	-0.9	0.06	0.00
10	5	0.0	0.00	0.00	-0.6	0.05	0.00
10	6	0.0	0.00	0.00	-0.0	0.00	0.00
10	7	-0.7	0.04	0.00	-0.0	0.00	0.00
10	8	1.3	0.07	0.00	-0.0	0.00	0.00
10	9	0.1	0.08	0.00	-0.3	0.09	0.00
10	10	-0.5	0.12	0.00	-0.0	0.00	0.00

Table 7: Statistics of Data Sets relative to GSFC(12/83)
Units are nT.

		B	X	Y	Z
Dawn data					
	RMS	6.8	8.9	8.3	7.3
	Mean	.6	.2	-.8	-4.6
	Sigma	6.8	8.9	8.3	5.7
Dusk data					
	RMS	8.4	12.8	14.2	9.8
	Mean	-1.6	-3.5	4.3	-.7
	Sigma	8.3	12.3	13.5	9.8
Merged dawn and dusk (corrected dusk data)	RMS	7.0	8.2	8.1	6.9
	Mean	.5	-1.1	1.3	-3.7
	Sigma	7.0	8.1	8.0	5.9
Observatory Data (1978.5 - 1982.5 with biases)	RMS	12.9	16.9	9.4	14.4
	Mean	-.4	-.1	.02	-.2
	Sigma	12.9	16.9	9.4	14.4
(1978.5 - 1982.5 without biases)	RMS	396.7	212.8	211.5	379.9
	Mean	4.1	3.1	13.7	-16.2
	Sigma	396.7	212.8	211.0	379.6

Table 8: Comparison of g_1^0 for several Magsat models

Model	Epoch	g_1^0(nT)	Difference from GSFC(12/83) at same epoch (nT)	Reference
MGST(6/80)	1979.85	-29989.6	-.9	Langel et al., 1980
GSFC(9/80)	1980.0	-29987.9	-3.7	Langel et al., 1982
IGRF 1980	1980.0	-29988.0	-3.6	Peddie, 1982

Table 9: Statistics of Data Sets relative to IGRF80 with external field parameters from GSFC(12/83). Units are nT.

		B	X	Y	Z
Dawn data					
	RMS	15.7	11.7	11.0	13.3
	Mean	-4.6	-.6	-.7	-4.2
	Sigma	15.0	11.7	11.0	12.6
Dusk data					
	RMS	16.0	15.0	16.2	14.9
	Mean	-7.1	-4.5	4.2	-.7
	Sigma	14.3	14.3	15.7	14.9
Merged dawn and dusk (corrected dusk data)	RMS	14.8	11.6	11.0	13.2
	Mean	-4.1	-2.0	1.3	-3.6
	Sigma	14.2	11.4	10.9	12.7
Observatory Data (1978.5 - 1982.5 with biases)	RMS	26.3	24.8	19.9	30.9
	Mean	-3.8	-5.6	3.9	.6
	Sigma	26.0	24.2	19.5	30.9
(1978.5 - 1982.5 without biases)	RMS,	398.4	211.8	214.0	381.7
	Mean	.6	-2.3	17.7	-15.4
	Sigma	398.4	211.8	213.3	381.4

TABLE 10: Secular variation coefficients from selected models

year	symbol in figure	reference	$\dot{g}_1^o$	$\dot{h}_1^1$	$\dot{g}_2^o$	$\dot{h}_2^1$
1960	X	Hurwitz and Fabiano (1969)	17.6	- 0.5	-23.5	-12.9
1960	□	Malin (1969)	16.4	0.5	-22.2	-15.0
1965	X	Hurwitz et al. (1974)	23.1	- 4.56	-24.4	-10.4
1965	□	Barraclough et al. (1978)	20.8	- 4.4	-22.4	- 9.2
1967	X	Hurwitz et al. (1973)	24.0	- 8.4	-23.3	- 6.2
1967.5	.	Peddie and Fabiano (1982)	22.8	- 9.4	-24.0	- 5.2
1971	X	Peddie and Fabiano (1976)	24.4	-10.3	-24.9	- 3.1
1972.5	.	Peddie and Fabiano (1982)	22.8	-12.6	-23.2	- 4.4
1977.5	.	Peddie and Fabiano (1982)	21.4	-14.0	-18.8	-11.6
1980	I	Peddie (1982); IGRF 1980	22.4	-15.9	-18.3	-12.7
1980	G	GSFC(12/83)	26.5	-16.0	-17.8	-15.0

Table 11: Statistics relating to anomaly bias determination

Component	Rms of biases from GSFC(9/80), nT	Rms of biases from GSFC(12/83), nT	Rms of bias differences
X	292	210	32
Y	344	199	38
Z	507	366	50

Figure Captions

Figure 1: Difference between computed fields from the dawn model and the dusk model at 500 km altitude. Units are nT. (a) X-component. (b) Z-component.

Figure 2: Difference between computed fields from the dawn model and the corrected dusk model at 500 km altitude. Units are nT. (a) X-component. (b) Z-component.

Figure 3: Secular variation at 1980 from the GSFC(12/83) model. (a) $\dot{B}$, (b) $\dot{X}$, (c) $\dot{Y}$, (d) $\dot{Z}$, (e) $\dot{H}$. Units are nT/yr.

Figure 4: Distribution of Magnetic Observatories used in the GSFC(12/83) solution.

Figure 5: X , Y and Z component values from observatories for 1978-1982. Data points are annual means; solid line is computed from GSFC(12/83); dashed line is computed from IGRF 1980. The model components (solid and dashed lines) for X , Y and Z are identified by (X) , (Y) , and (Z) , respectively. Both models use the observatory biases computed with GSFC(12/83). Units are nT. (a) Boulder, (b) Guam, (c) Huancayo, (d) Muntinlupa, (e) Tromso.

Figure 6: Spherical harmonic coefficients from selected models versus time from 1960-1980. Units are nT. The selected models are listed in Table 10. (a) $\dot{g}_1^0$, (b) $\dot{g}_2^0$, (c) $\dot{h}_1^1$, (d) $\dot{h}_2^1$.

Figure 1a

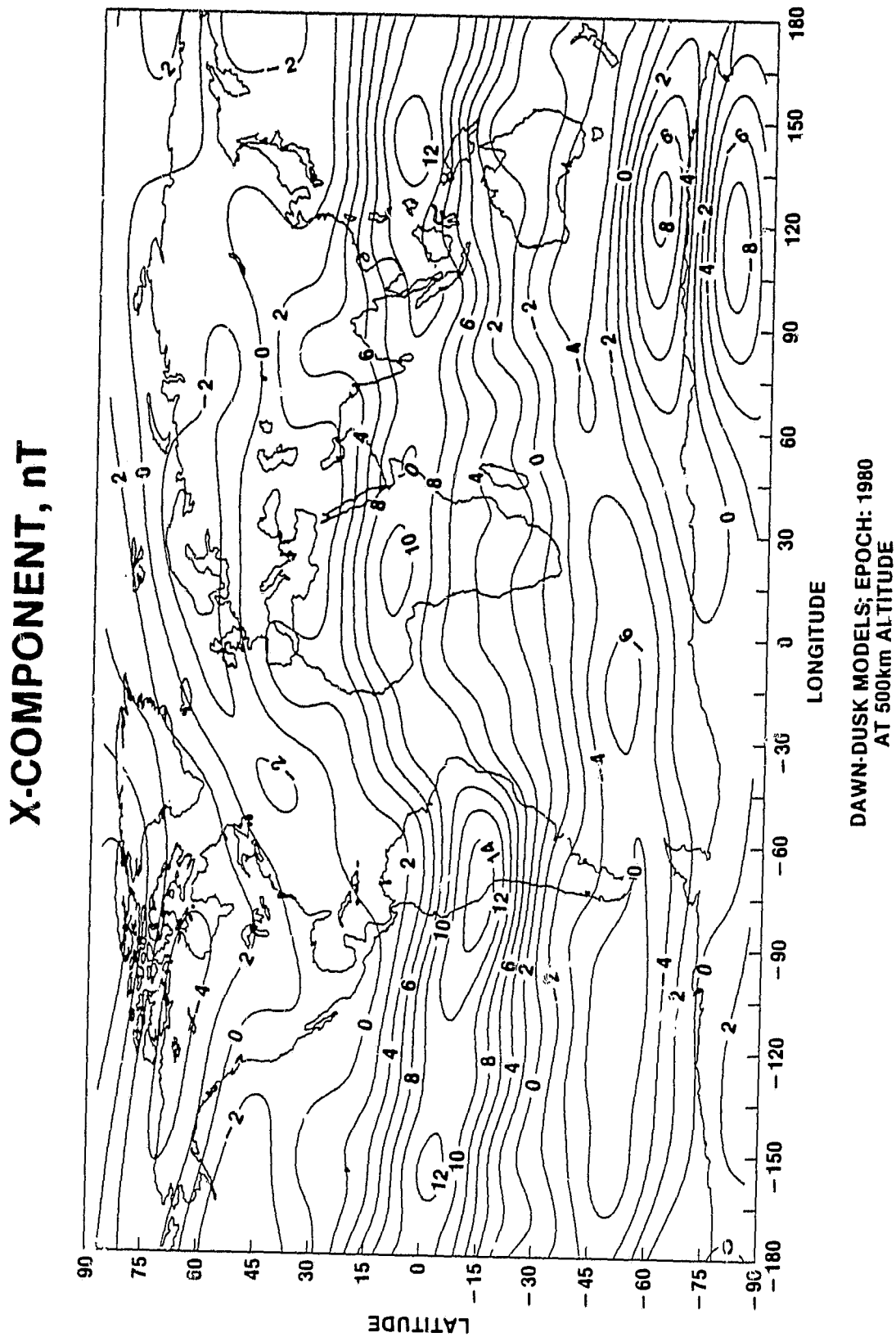

Figure 1b

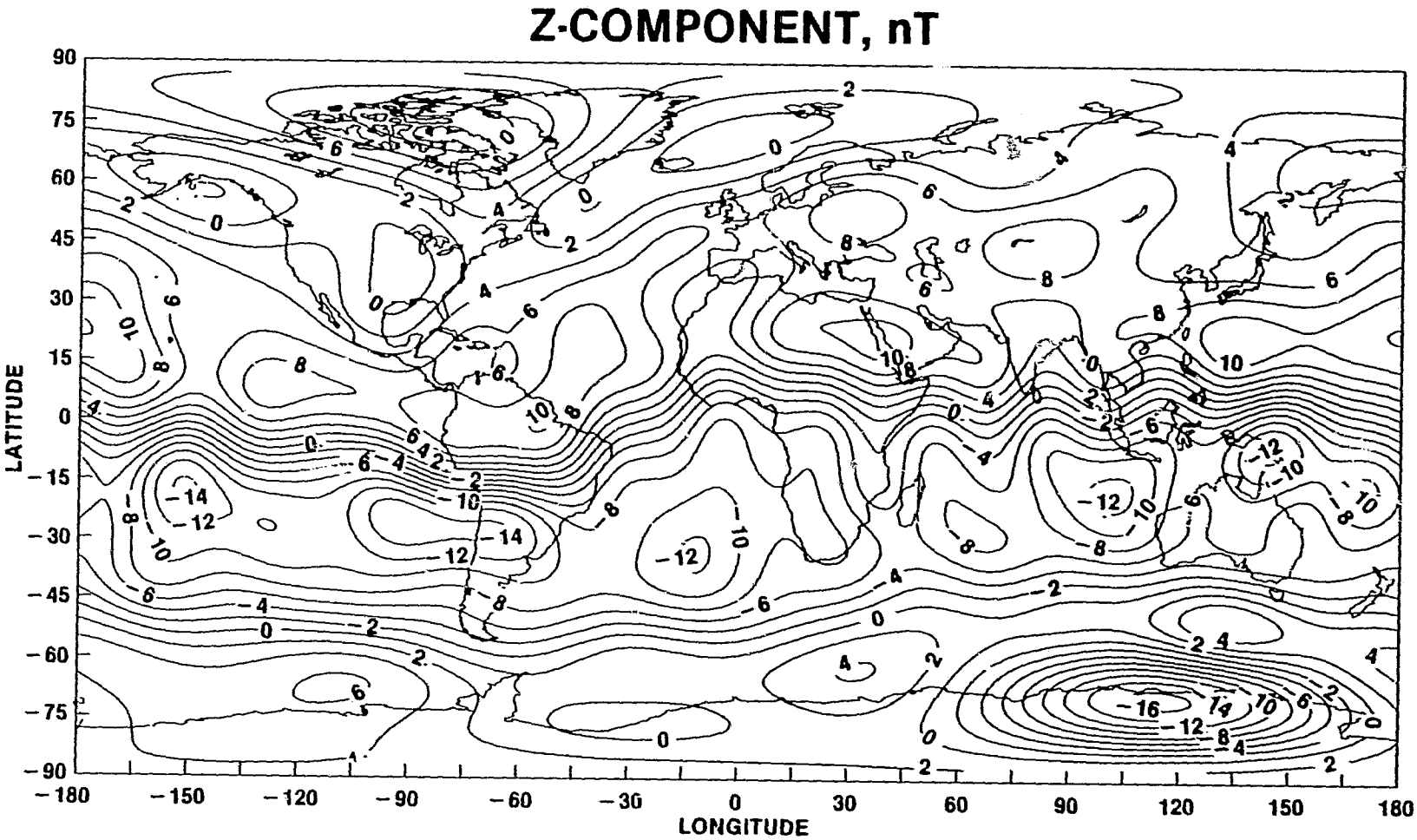

DAWN-DUSK MODELS; EPOCH: 1980
AT 500km ALTITUDE

Figure 2a

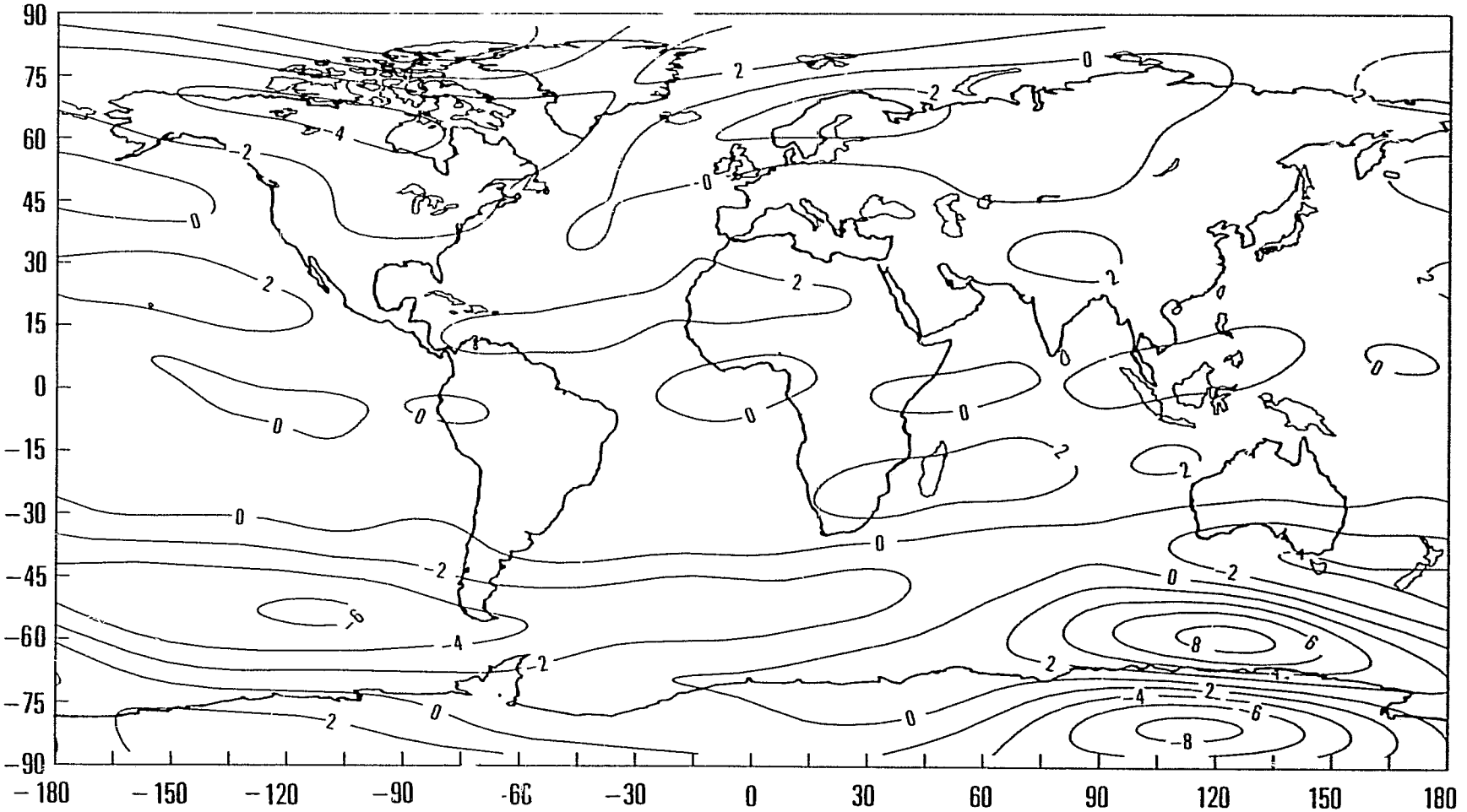

Figure 2b

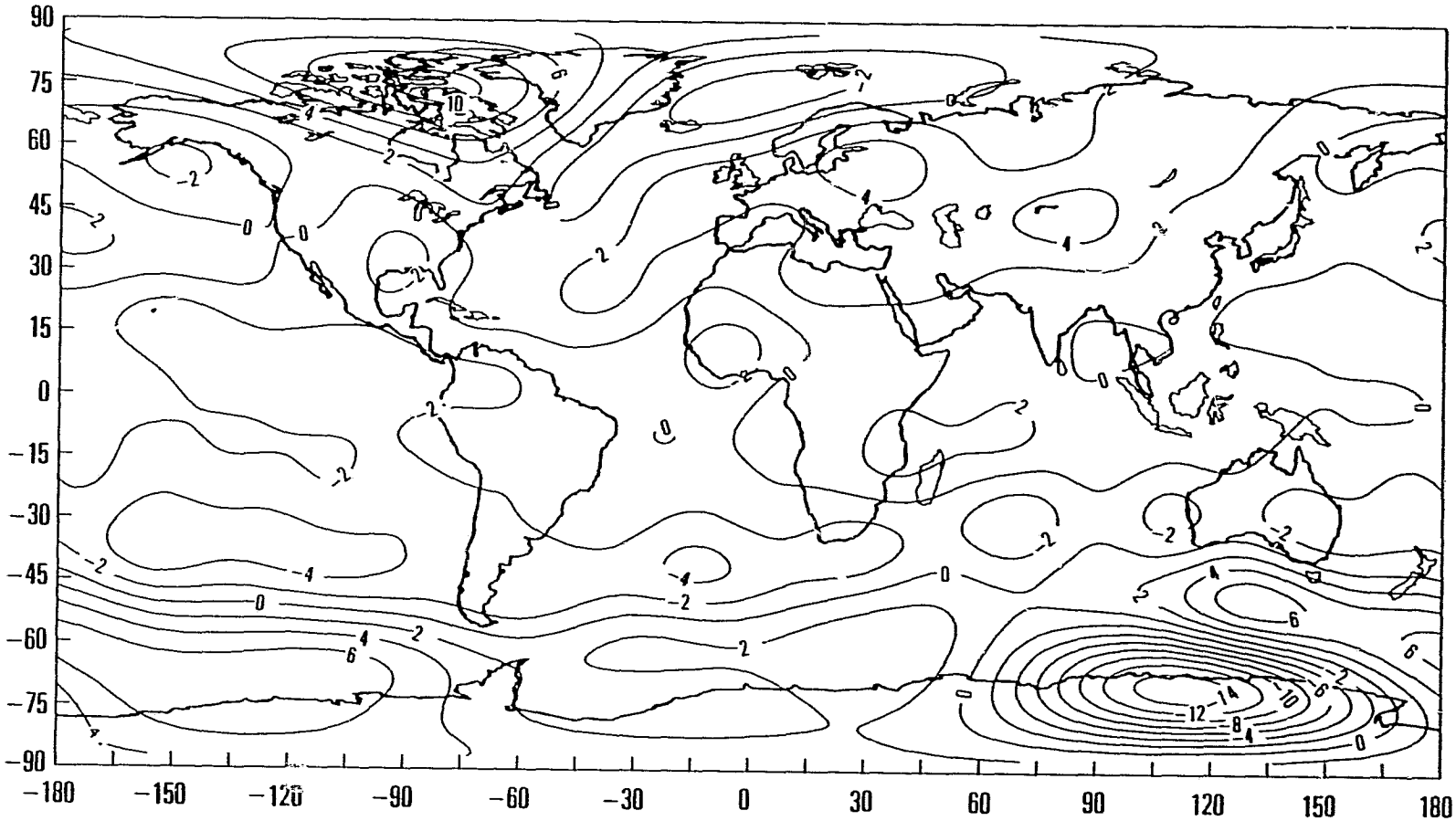

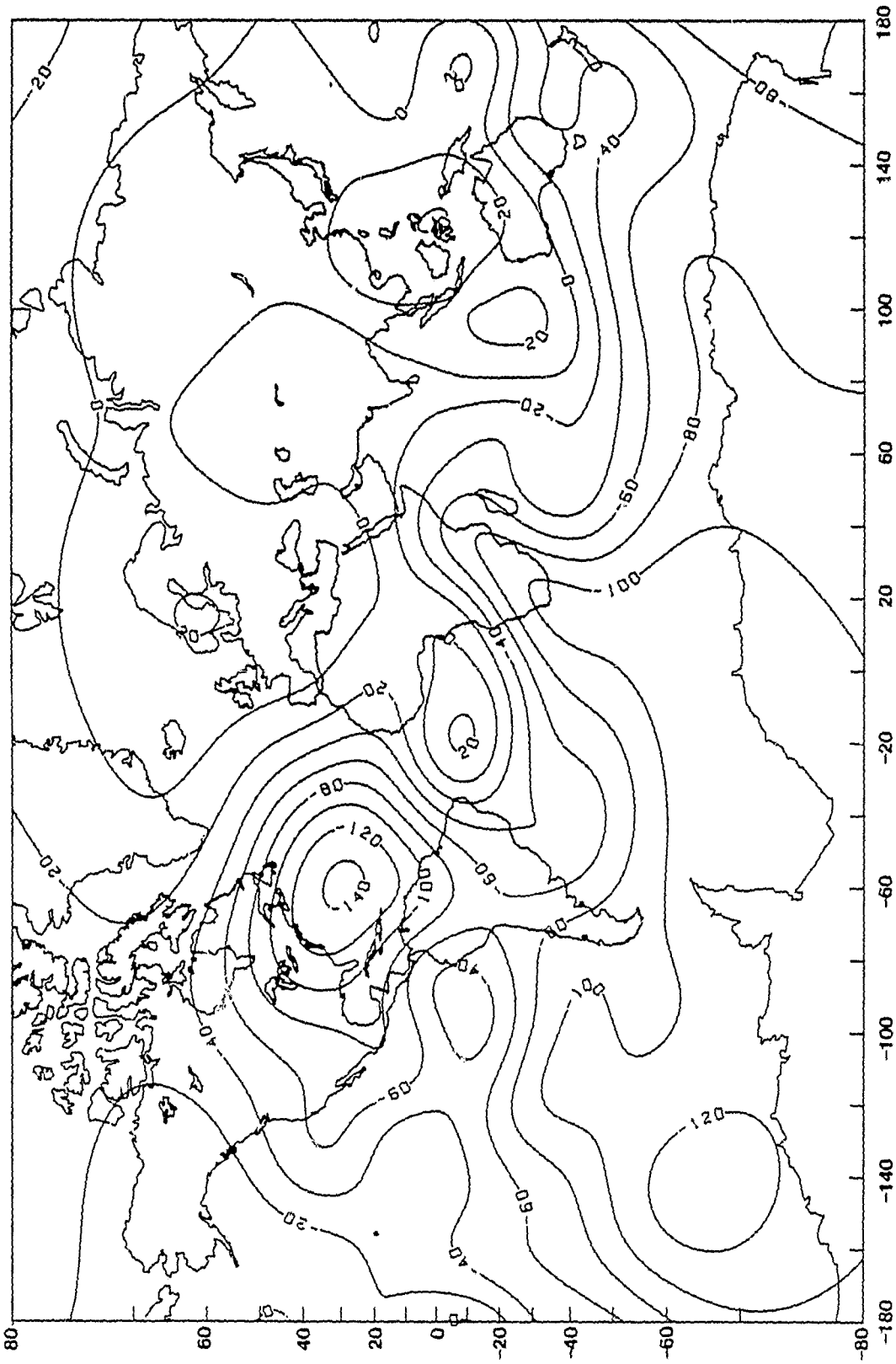

Figure 3a

Figure 3b

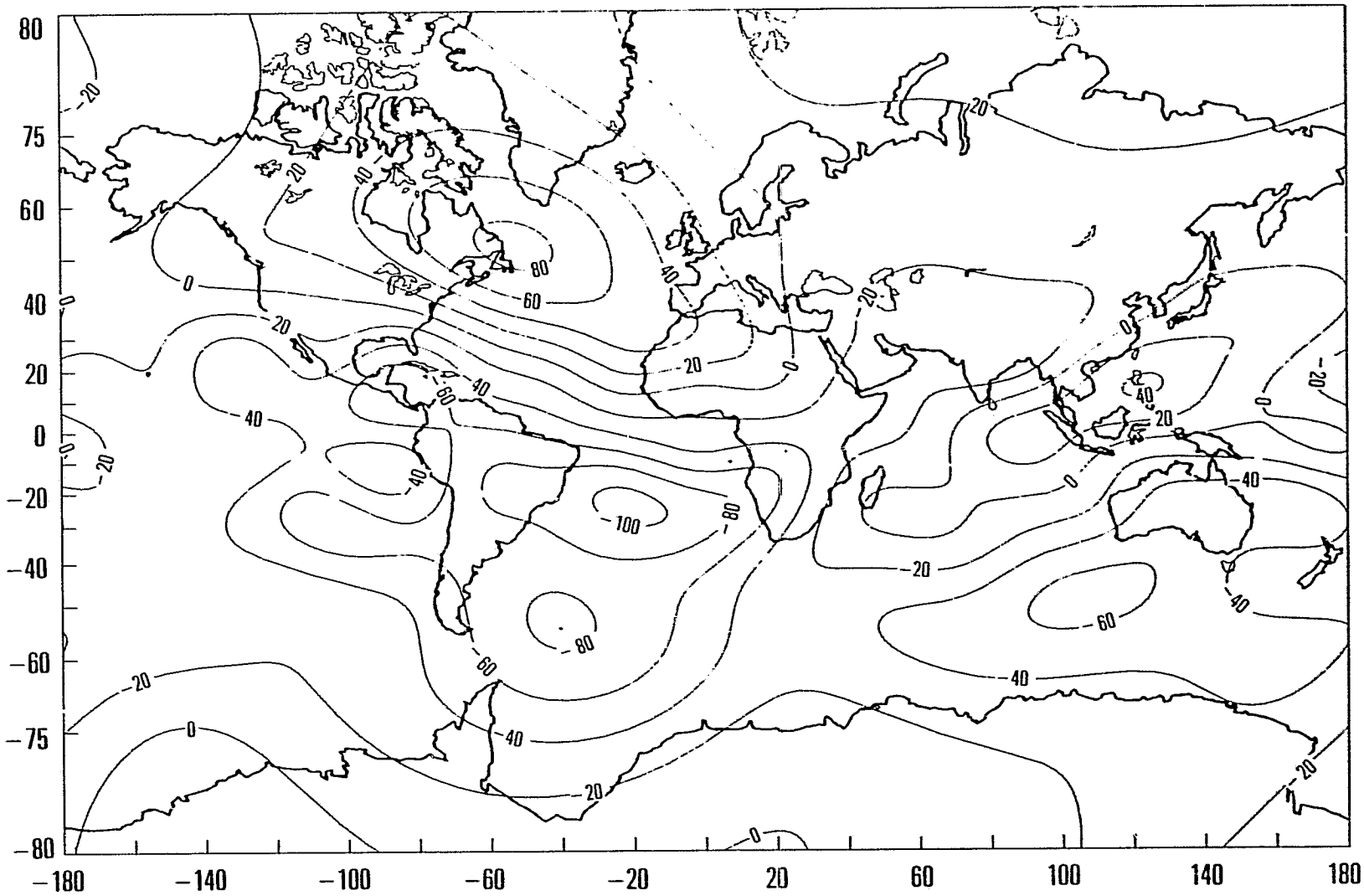

Figure 3c

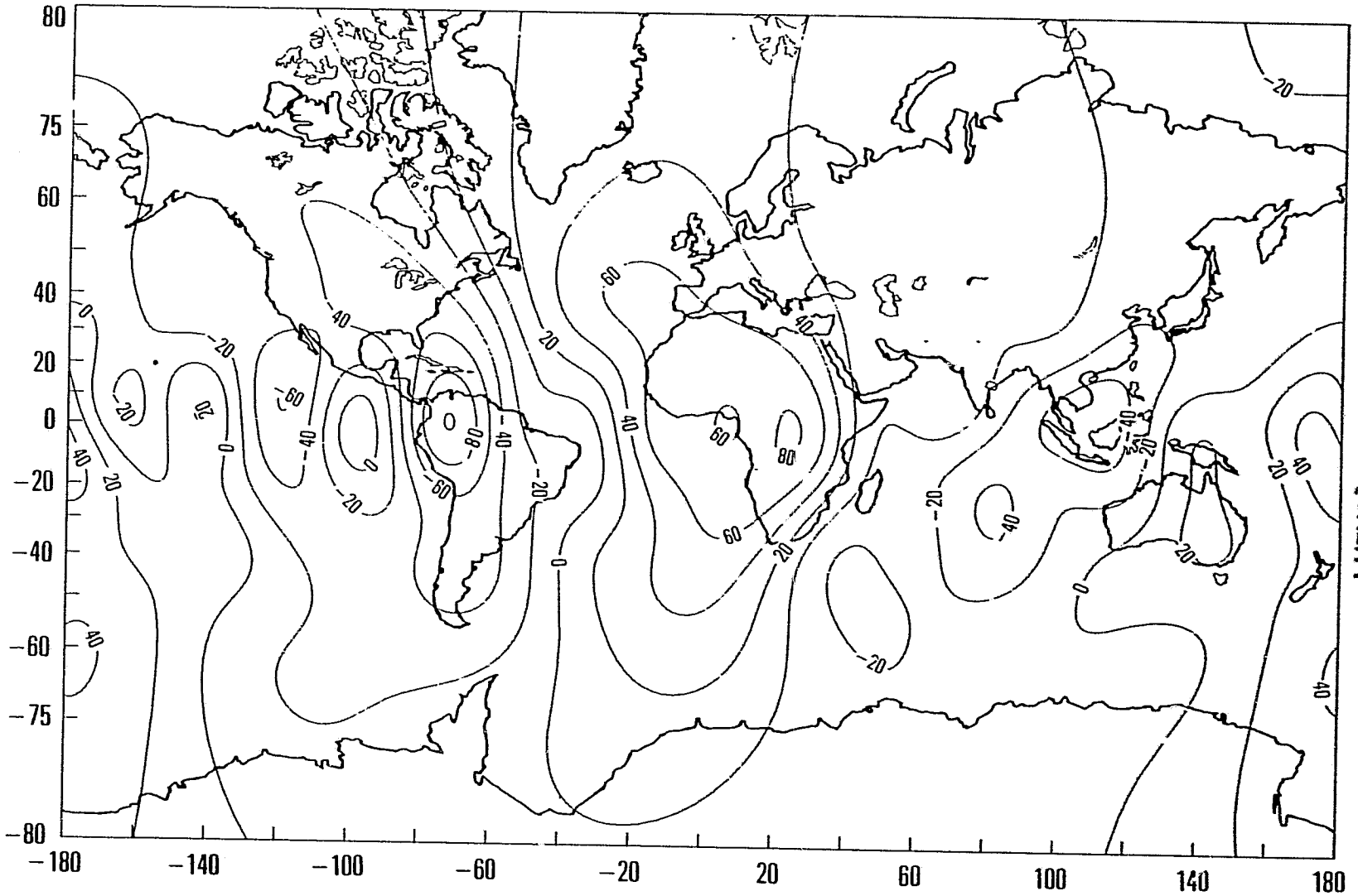

Figure 3d

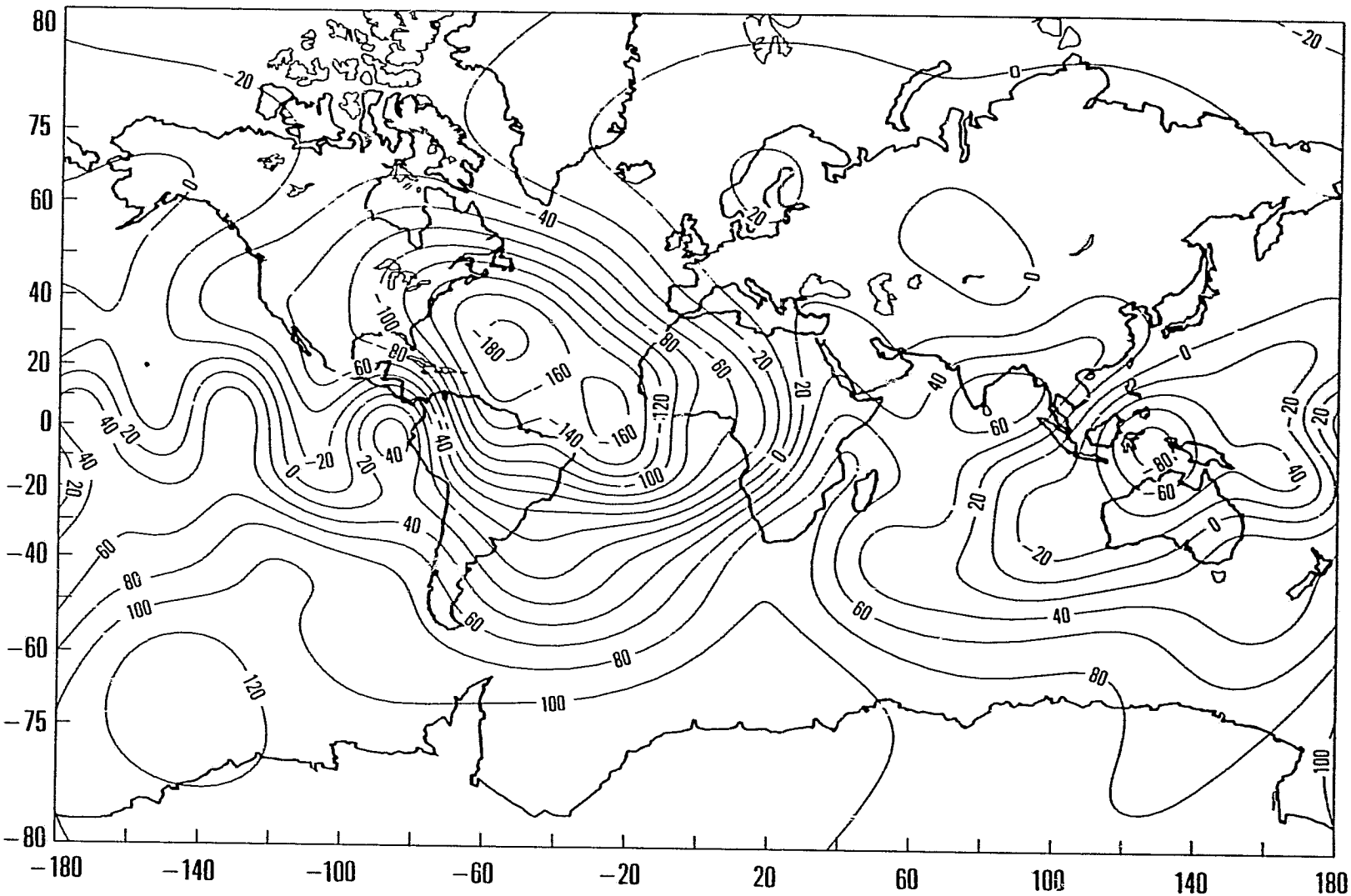

Figure 3e

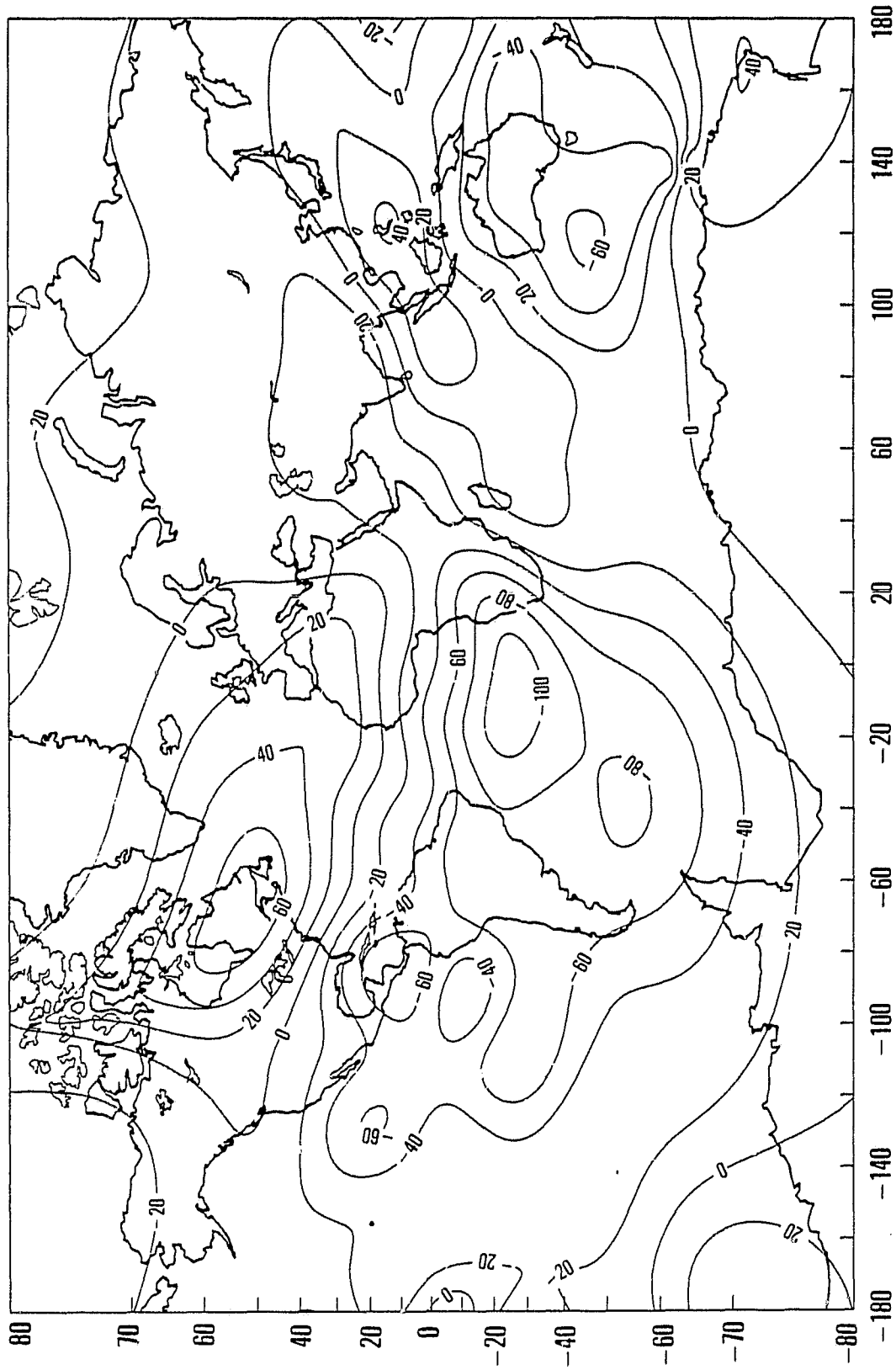

Figure 4

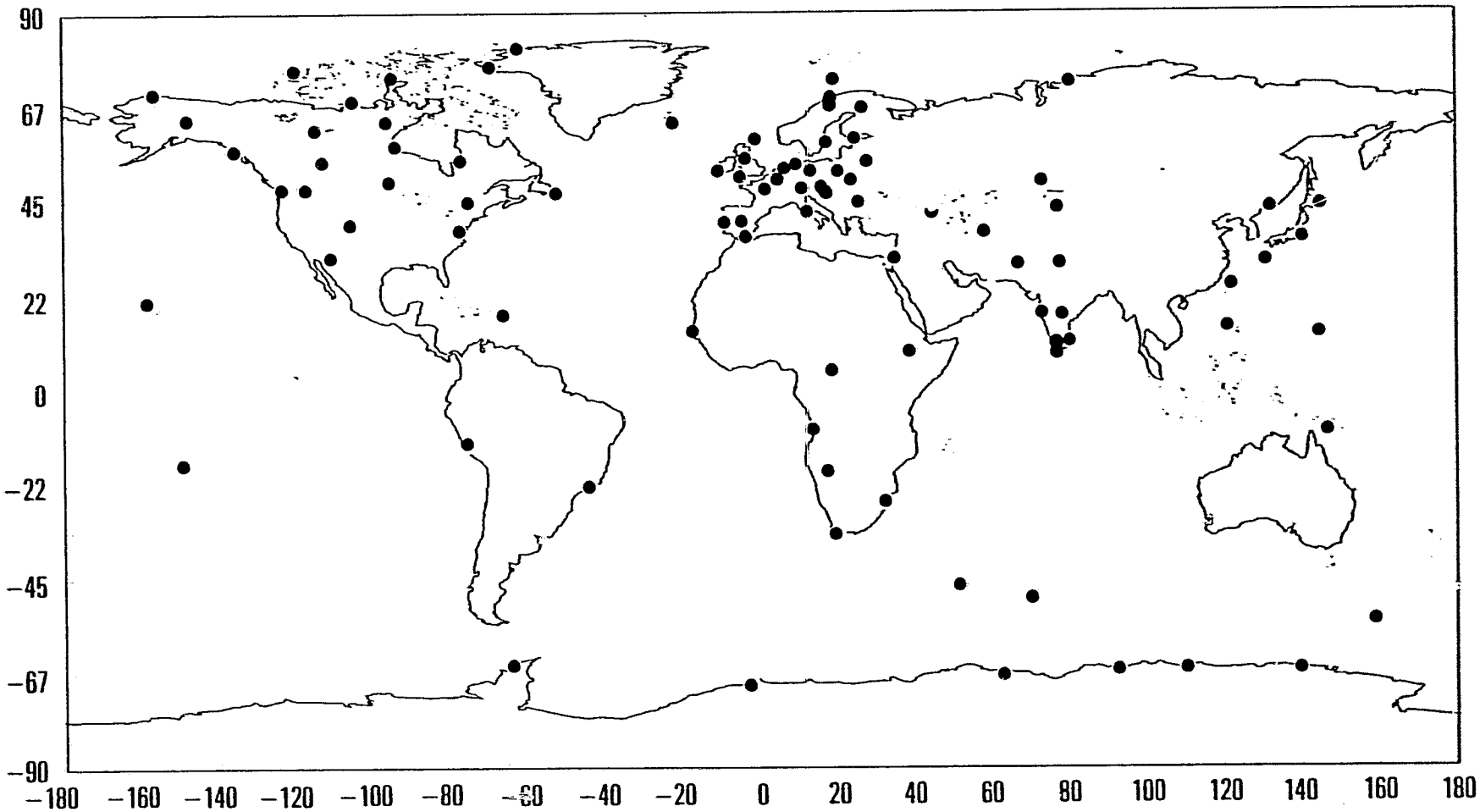
90
67
45
22
0
−22
−45
−67
−90
−180
−160
−140
−120
−100
−80
−60
−40
−20
0
20
40
60
80
100
120
140
160
180

Figure 5a

BOULDER

LAT 40.14 LON -105.24 ALT 1.65 KM

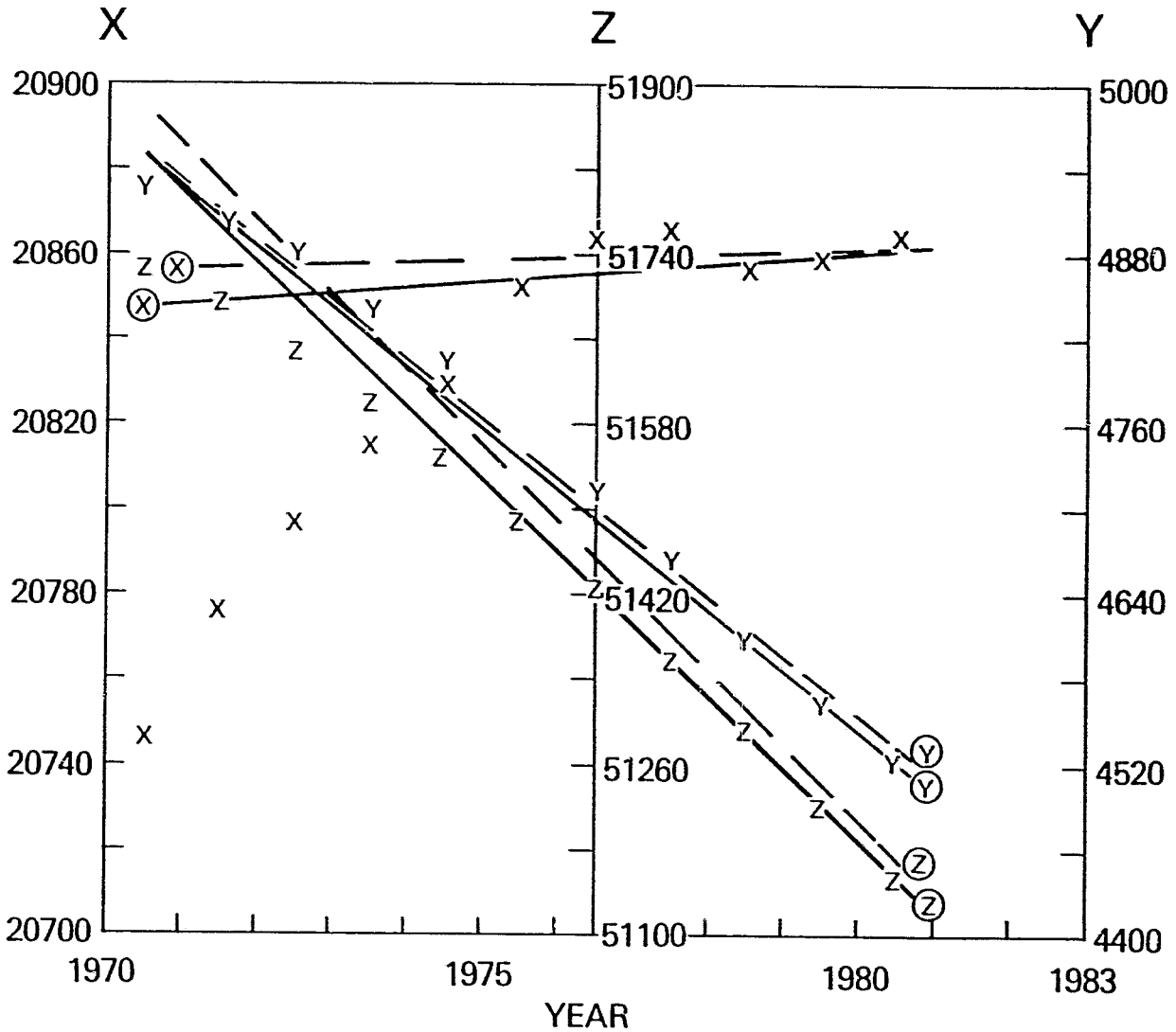

Figure 5b

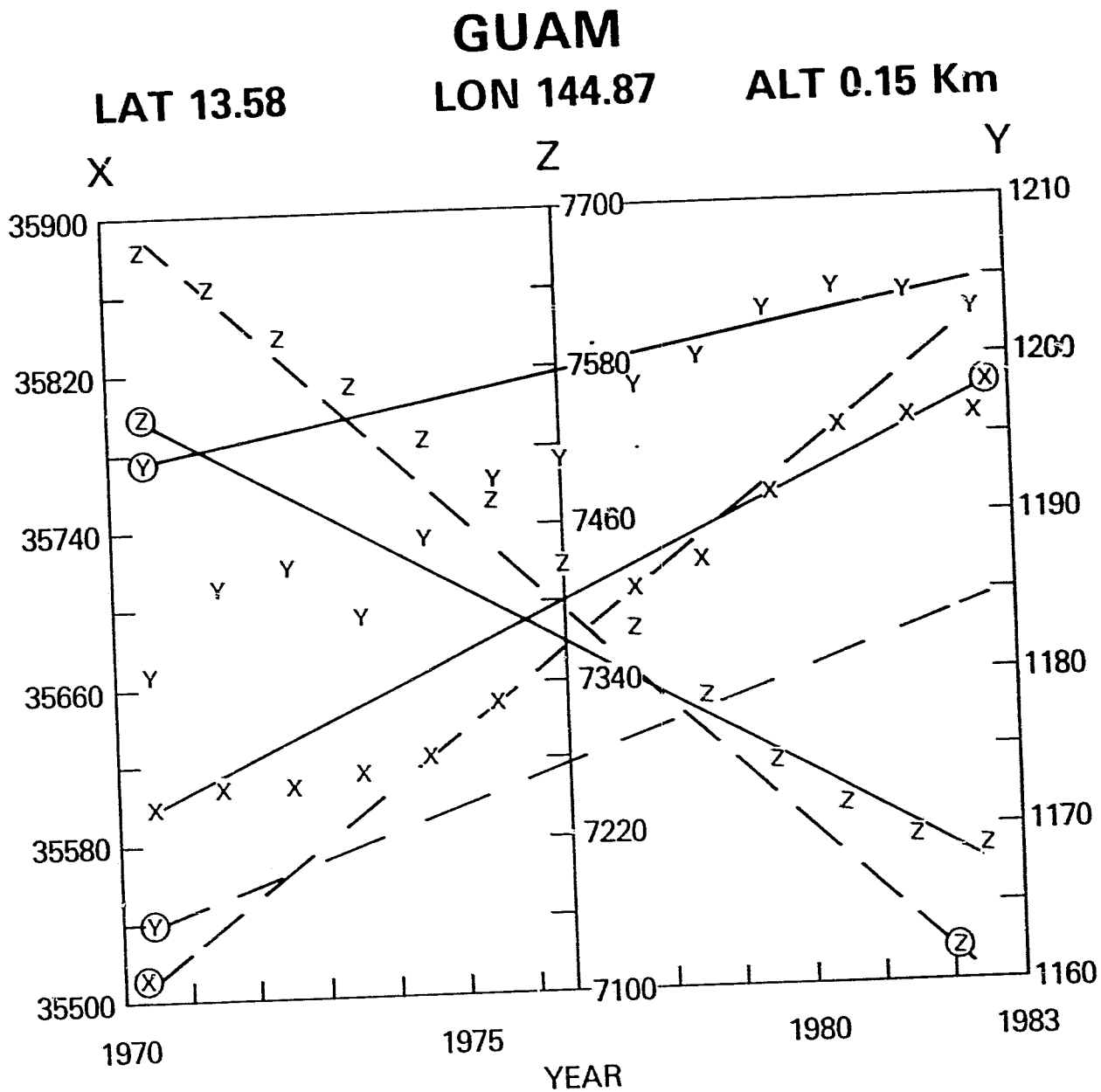
GUAM
LAT 13.58
LON 144.87
ALT 0.15 Km
X
Z
Y
35900
35820
35740
35660
35580
35500
7700
7580
7460
7340
7220
7100
1210
1200
1190
1180
1170
1160
1970
1975
1980
1983
YEAR

Figure 5c

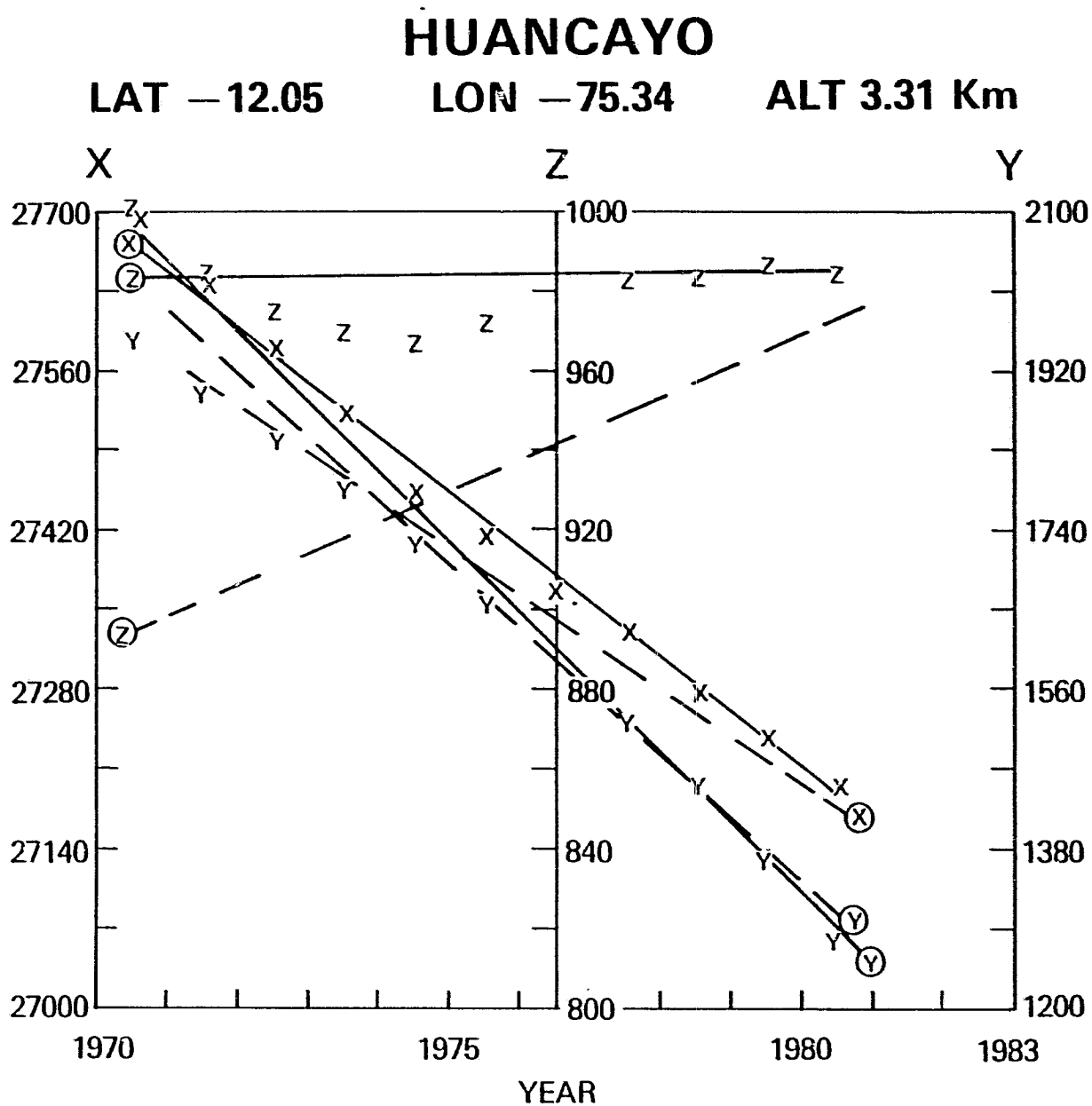
HUANCAYO
LAT −12.05
LON −75.34
ALT 3.31 Km
X
Z
Y
27700
27560
27420
27280
27140
27000
1000
960
920
880
840
800
2100
1920
1740
1560
1380
1200
1970
1975
1980
1983
YEAR

Figure 5d

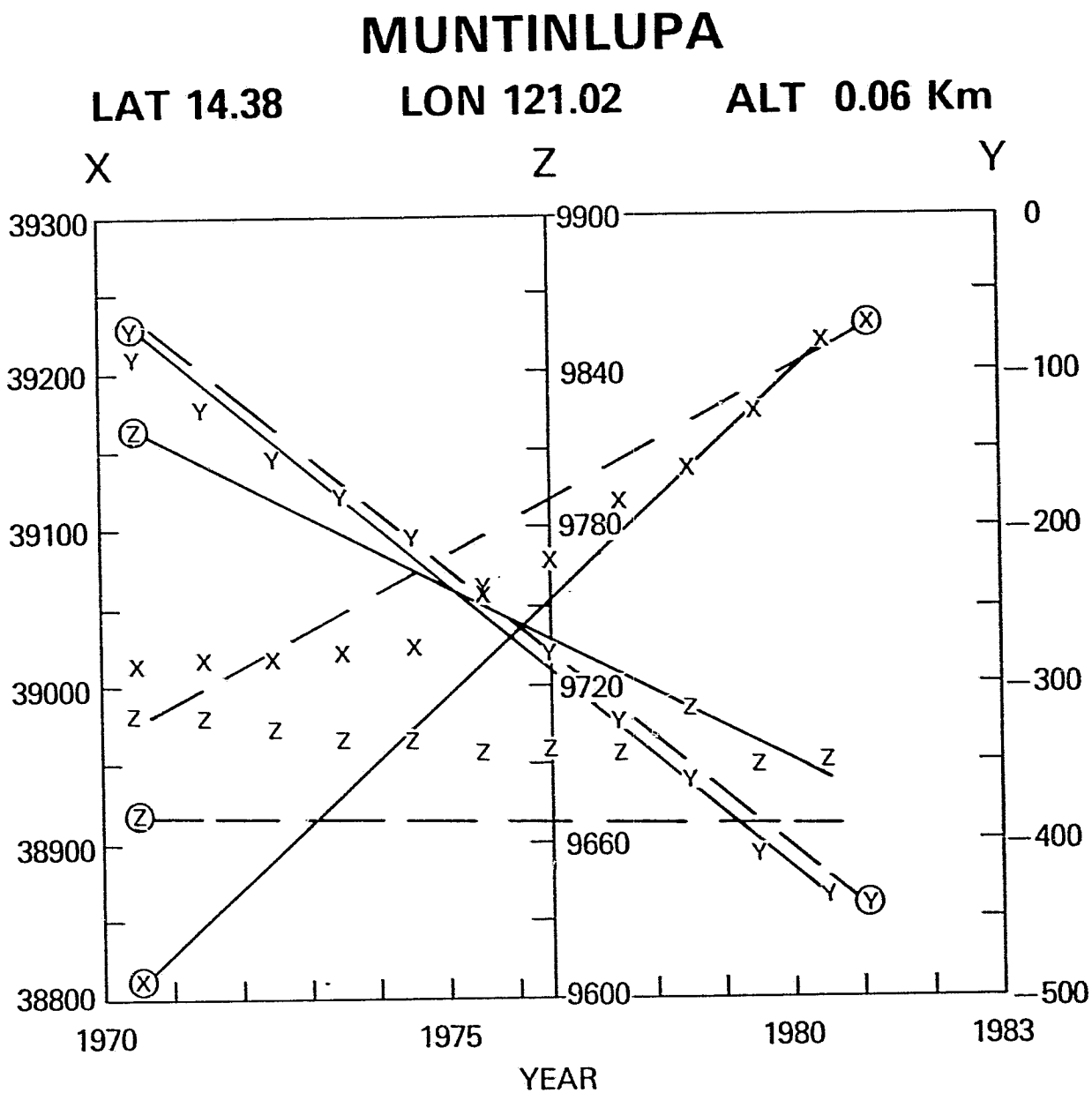
MUNTINLUPA
LAT 14.38
LON 121.02
ALT 0.06 Km
X
Z
Y
39300
39200
39100
39000
38900
38800
9900
9840
9780
9720
9660
9600
0
100
200
300
400
500
1970
1975
1980
1983
YEAR

Figure 5e

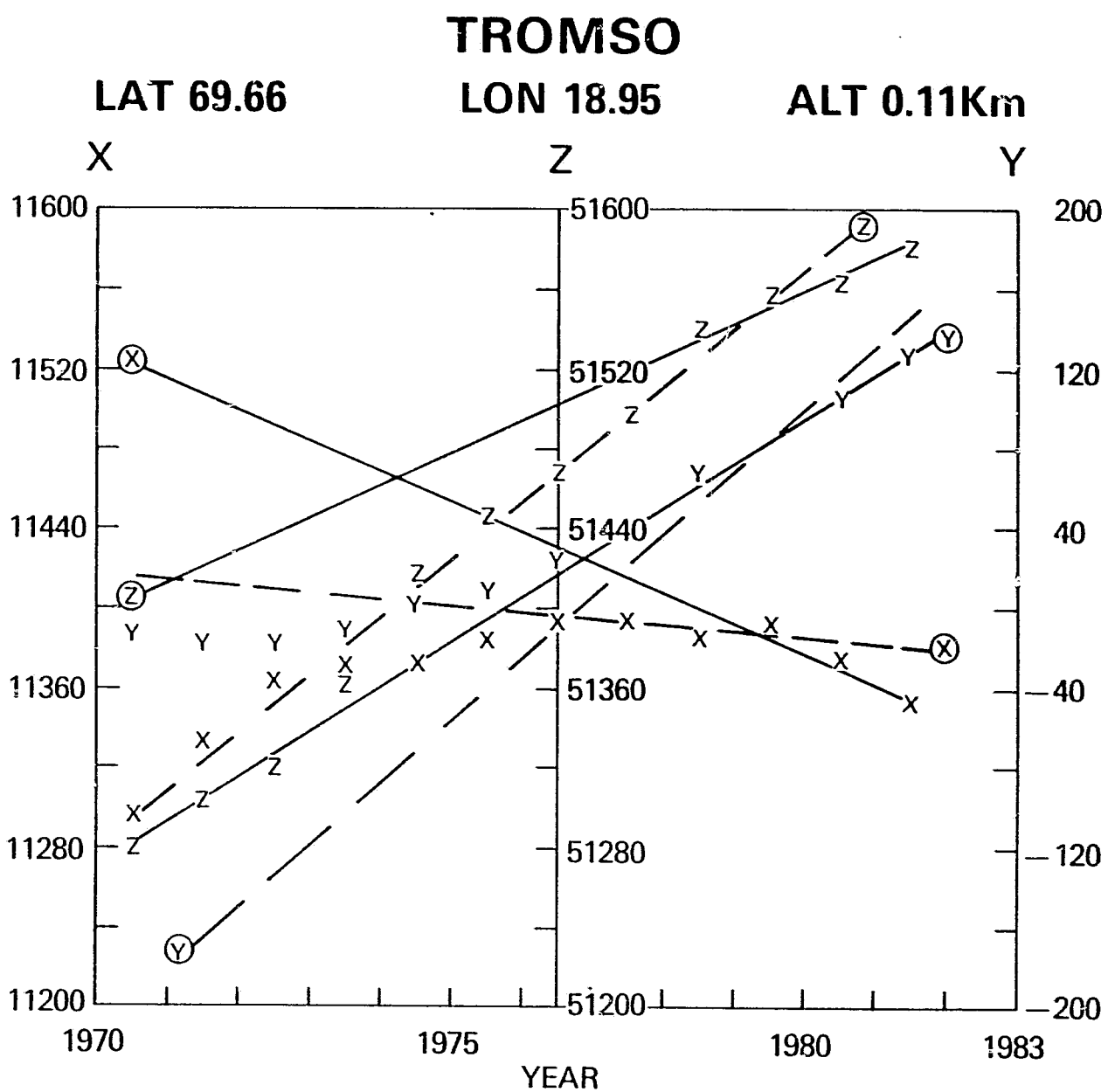

Figure 6a

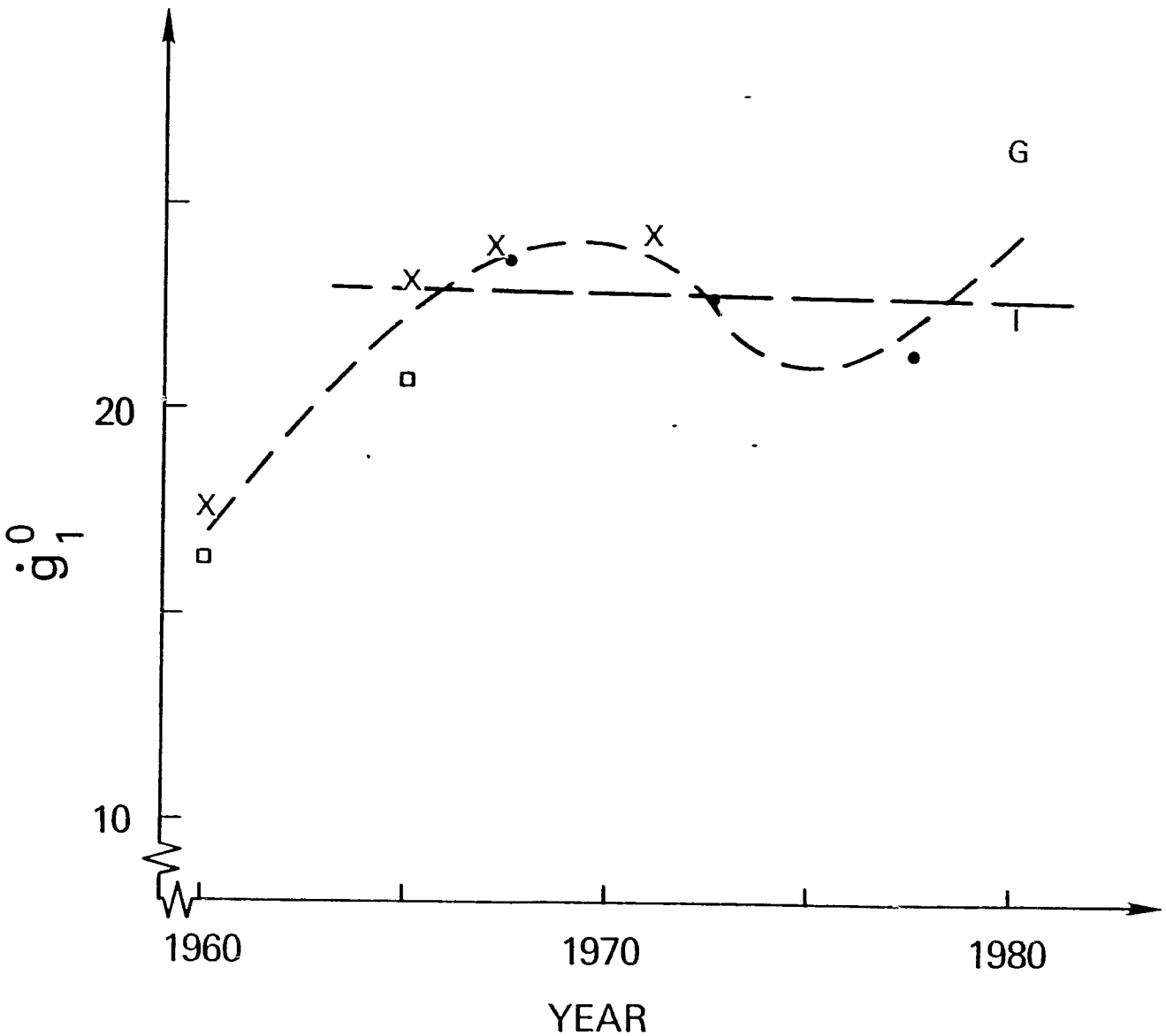

Figure 6b

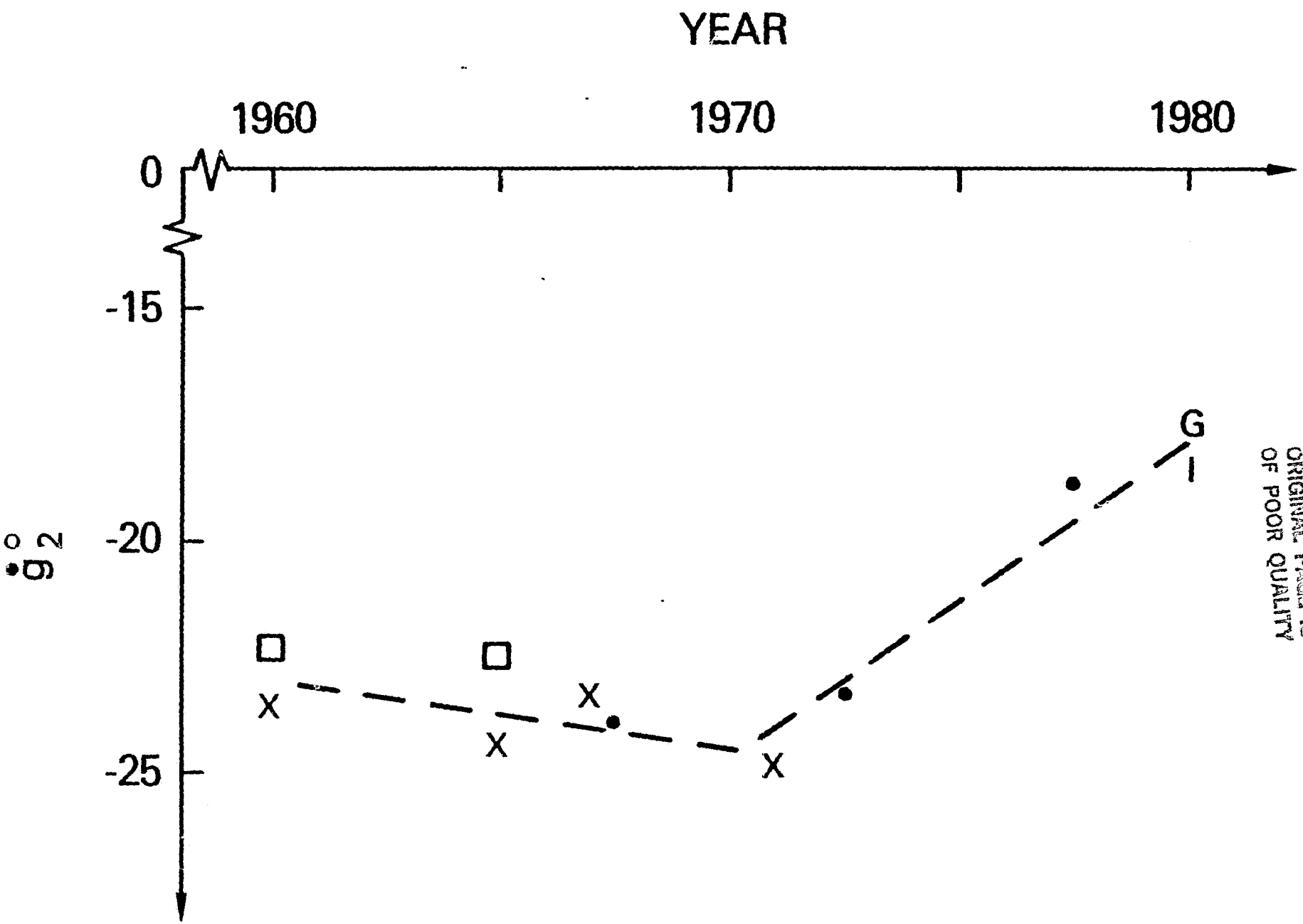

Figure 6c

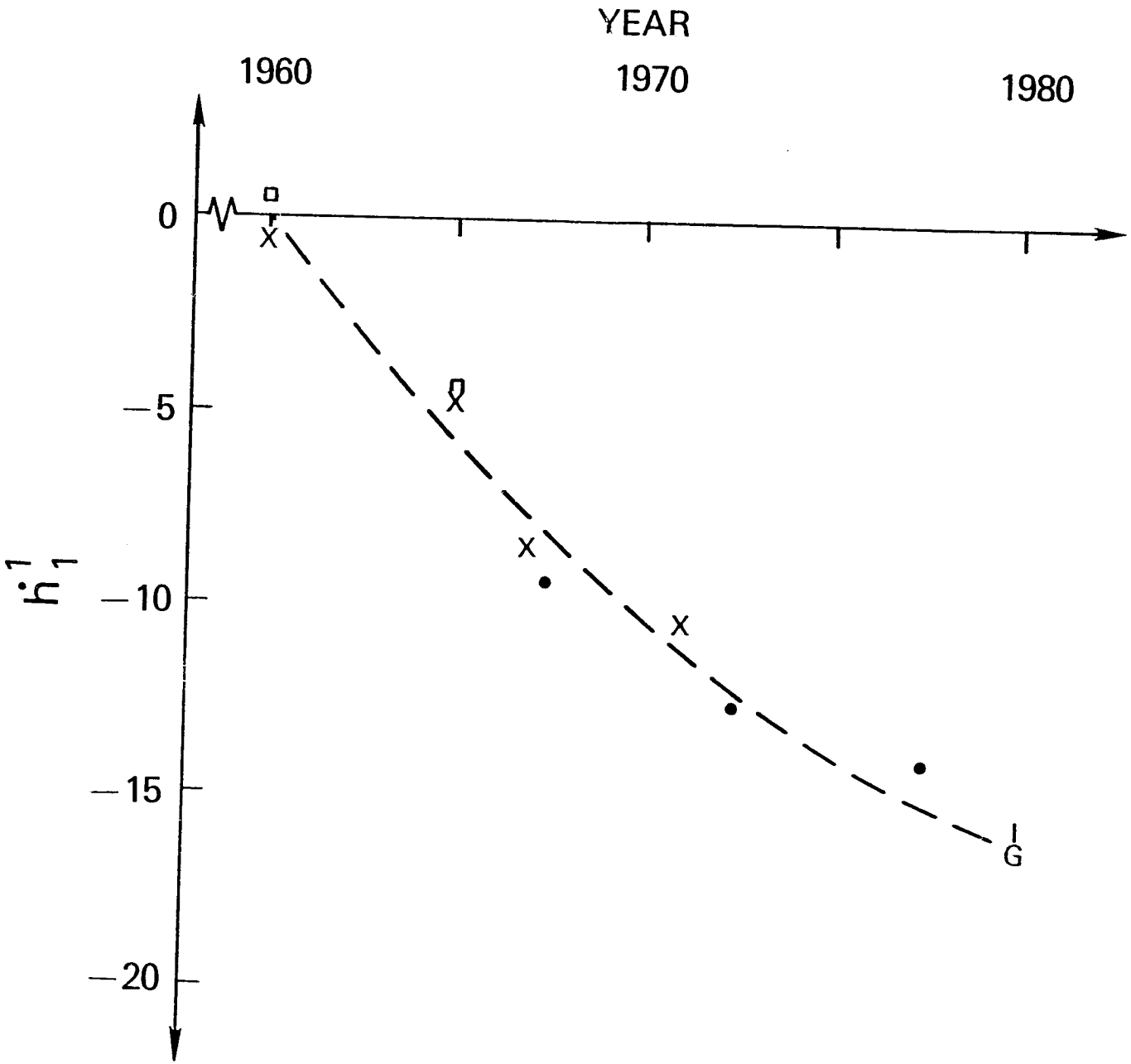

Figure 6d